

Phase diagram of Josephson junction between s and s_{\pm} superconductors in dirty limit

A. E. Koshelev

Materials Science Division, Argonne National Laboratory, Argonne, Illinois 60439

(Dated: September 1, 2018)

The s_{\pm} state in which the order parameter has different signs in different bands is a leading candidate for the superconducting state in the iron-based superconductors. We investigate a Josephson junction between s and s_{\pm} superconductors within microscopic theory. Frustration, caused by interaction of the s -wave gap parameter with the opposite-sign gaps of the s_{\pm} superconductor, leads to nontrivial phase diagram. When the partial Josephson coupling energy between the s -wave superconductor and one of the s_{\pm} bands dominates, s -wave gap parameter aligns with the order parameter in this band. In this case the partial Josephson energies have different signs corresponding to signs of the gap parameters. In the case of strong frustration, corresponding to almost complete compensation of the total Josephson energy, a nontrivial time-reversal-symmetry breaking (TRSB) state realizes. In this state all gap parameters become essentially complex. As a consequence, this state provides realization for so-called ϕ -junction with finite phase difference in the ground state. The width of the TRSB state region is determined by the second harmonic in Josephson current, $\propto \sin(2\phi)$, which appears in the second order with respect to the boundary transparency. Using the microscopic theory, we establish a range of parameters where different states are realized. Our analysis shows insufficiency of the simple phenomenological approach for treatment of this problem.

I. INTRODUCTION

The discovery of superconducting iron pnictides and chalcogenides is one of the most remarkable recent achievements in the condensed-matter physics. A rapid progress in characterization of these materials and development of theoretical understanding has been reflected in several reviews^{1,2}. The key feature of these semimetallic materials is the multiple-band structure, the Fermi surface is composed of several electron and hole pockets located near different points of the Brillouin zone.

Superconductivity in the iron-based materials is likely to be unconventional. There is a theoretical consensus that the electron-phonon interaction is not strong enough to explain high transition temperatures.³ In several theoretical papers it was suggested that superconductivity is mediated by spin fluctuations leading to an unusual superconducting state in which the order parameter has opposite signs in the electron and hole bands (s_{\pm} state).⁴⁻⁸ Experimental verification of this theoretical proposal became one of the major challenges in the field. Probing the relative sign of the order parameter in different bands is not trivial and the structure of superconducting state has not been unambiguously established yet by experiment, even though several properties consistent with the s_{\pm} state have been revealed. An extensive critical review of experiments both in favor and against the realization of the s_{\pm} state in iron-based superconductors has been done recently in Refs. 2. Shortly, the main experiments supporting the s_{\pm} state include

- Observation by the inelastic neutron scattering of the resonant magnetic mode below the superconducting transition temperature.⁹ Such a mode is expected for the superconductors with the sign-changing order parameter. This mode was observed in almost all compounds and its frequency scales approximately proportional to the transition tem-

perature.

- Microscopic coexistence of antiferromagnetism and superconductivity demonstrated in some compounds within a narrow doping range, most clearly in $\text{Ba}[\text{Fe}_{1-x}\text{Co}_x]_2\text{As}_2$.^{10,11} For the case of the conventional s_{++} state in which the order parameter has the same sign in all bands, the spin-density wave (SDW) has a strong pair-breaking effect on the bands connected with the SDW ordering wave vector. Such direct pair breaking is absent if the order parameter in such bands has opposite signs meaning that the SDW is much more compatible with the s_{\pm} state than with s_{++} one.¹²
- The magnetic field dependence of the quasiparticle interference peaks studied by scanning tunneling spectroscopy in $\text{FeSe}_x\text{Te}_{1-x}$.¹³

On the other hand, discovery of the iron selenide compounds *without hole band* and with rather high transition temperatures, up to 30K¹⁴, questioned universality of the s_{\pm} state for all iron-based superconductors. Also, it occurs that the iron-based superconductors are quite stable with respect to disorder. As for the s_{\pm} state the inter-band scattering is pair breaking, stability with respect to disorder is frequently used as an argument against this state. Therefore the structure of the order parameter in the iron-based superconductors is an unresolved issue.

One of the ways to probe unconventional superconductivity is to study Josephson junctions and proximity effects with conventional superconductors. In the case of contact between s -wave and s_{\pm} superconductors, frustration, caused by interaction of the s -wave gap parameter with the opposite-sign gaps of s_{\pm} superconductor leads to several anomalous features which were recognized and studied in several theoretical papers.¹⁶⁻²⁴ For example, proximity with s_{\pm} superconductor induces corrections to the density of states of s -wave superconductor which, in

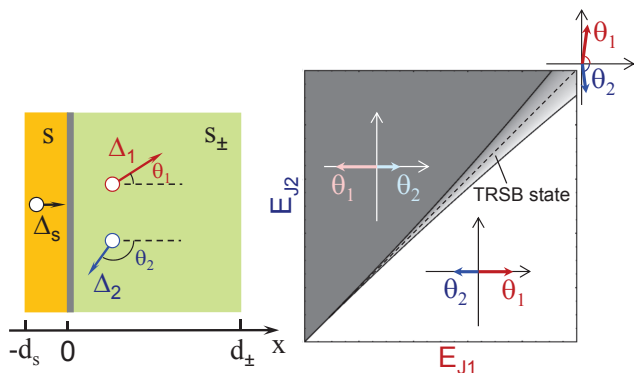


FIG. 1. *Left part:* A Josephson junction between s and s_{\pm} superconductors with the gap parameters for a general complex state. *Right part:* Generic phase diagram of such Josephson junction.

principle, allow to identify the signs of the order parameter in different bands of s_{\pm} superconductor.²² Particularly interesting is a possibility of a time-reversal symmetry breaking (TRSB) state^{16,19,21,23} in the parameter range where the partial Josephson coupling energies between s -superconductor and different s_{\pm} bands almost exactly compensate each other. Existing experiments on Josephson junctions between iron-based and conventional superconductors have been reviewed in Ref. 25. No anomalous features, however, have been reported so far.

For experimental realization of the TRSB state it is important to establish range of parameters where such state can be expected. Up to now this state was studied using mostly phenomenological models which are not rigorously justified. The purpose of this paper is to develop microscopic description of transition between the aligned and TRSB states. The paper is organized as follows. In Sec. II we present general consideration of the transition between the aligned and TRSB state in the region where the partial Josephson energies almost compensate each other. It is known that the width of the TRSB region is determined by the second harmonic of the Josephson current, which in our situation appears in the second order with respect to the coupling between superconductors. In Sec. III we present the microscopic equations and boundary conditions describing the contact between s -wave and s_{\pm} superconductors in dirty limit considered in this paper. In Sec. IV we consider corrections to the Green's functions and gap parameters induced by the interface. Computation details of these corrections are presented in Appendix A. The proximity-induced corrections to the Green's function determine the second harmonic in the Josephson current, which is considered in Sec. V. We present both general formulas for different contributions to the second harmonic and simple analytical results for the most relevant limiting cases. We also reveal the dominating contribution to the second harmonic. Using these results we analyze in Sec. VI the width of the TRSB region and its shrinking with

increasing temperature. Finally, in Sec. VII we consider proximity-induced corrections to the density of states of the s -wave superconductor within the TRSB region.

II. GENERAL CONSIDERATION OF THE TRANSITION REGION IN THE WEAK-COUPLING CASE

We consider the Josephson junction between s -wave and two-band s_{\pm} superconductors, see Fig. 1 (left). In the weak-coupling limit this system is characterized by the partial Josephson coupling energies between s -superconductor and s_{\pm} bands, $E_{J\alpha}$ with α being the band index. Typically, the s -wave gap parameter aligns along the s_{\pm} gap with which it has larger coupling energy. In this aligned state the partial Josephson coupling energies are positive and negative for the aligned and anti-aligned bands correspondingly. Nontrivial behavior is expected in the case of strong frustration when the total Josephson energy is close to zero. This happens when absolute values of the Josephson energies for the opposite-sign bands are close, $|E_{J1}| \approx |E_{J2}|$. Phenomenologically, the phase diagram can be described by the model of the frustrated Josephson junction considered in several papers¹⁶ which provides correct qualitative description. However, in general, this model does not describe the system quantitatively, because, ignoring the fermionic degrees of freedom in the s_{\pm} superconductor, it does not treat correctly its interband energy. For the weak-coupling regime, however, the transitional region between the two aligned states can be treated following the same reasoning as for the transition between 0 and π junctions, see, e.g., Refs. 18 and 26. In the vicinity of transition the linear approximation for the coupling between the superconductors becomes insufficient and the total Josephson energy can be represented as

$$\mathcal{E}(\phi) = (E_{J1} - E_{J2})(1 - \cos \phi) + \frac{E_J^{(2)}}{2}(1 - \cos 2\phi), \quad (1)$$

where ϕ is the phase difference between Δ_s and Δ_1 and the term $E_J^{(2)}$ appears in the second order with respect to the boundary transparency. This corresponds to the Josephson current

$$j(\phi) = (j_{J1} - j_{J2}) \sin \phi + j_J^{(2)} \sin 2\phi \quad (2)$$

with $j_{J\alpha} = (2\pi c/\Phi_0)E_{J\alpha}$. The intermediate TRSB state exists only if the sign of the second-harmonic is negative $E_J^{(2)}, j_J^{(2)} < 0$. In this case in the region $|j_{J1} - j_{J2}| < 2|j_J^{(2)}|$ the ground-state phase difference is given by

$$\cos \phi_0 = (j_{J1} - j_{J2}) / (2|j_J^{(2)}|). \quad (3)$$

It smoothly transforms between 0 and π when the difference $j_{J1} - j_{J2}$ changes from $2|j_J^{(2)}|$ to $-2|j_J^{(2)}|$. Therefore the TRSB state also provides realizations of so-called ϕ -junction²⁷ in which a finite phase difference exists in

ground state leading to several anomalous properties. In the case $E_J^{(2)}, j_J^{(2)} > 0$ the transition between the two aligned states is of the first order and the TRSB state is not realized.

The simplest phenomenological description is the frustrated Josephson junction model in which the tilt of the relative phase between two gap parameters of s_{\pm} superconductors is described by the energy $\mathcal{E}_{12} \cos(\theta_1 - \theta_2)$. In this model the amplitude of the second harmonic is given by

$$j_J^{(2)} = -\bar{j}_J \bar{E}_J / (2\mathcal{E}_{12})$$

with $\bar{j}_J = (j_{J1} + j_{J2})/2$ and $\bar{E}_J = (E_{J1} + E_{J2})/2$. Our further microscopic analysis shows that this result is only valid for a special situation of very weak coupling between the bands of the s_{\pm} superconductor. We will compute the second harmonic in general case within microscopic approach.

III. EQUATIONS AND BOUNDARY CONDITIONS

In this section we write down equations and boundary conditions for the simple microscopic model describing a “sandwich”, consisting of slabs of two-band s_{\pm} superconductor with thickness d_{\pm} and a single-band s -wave superconductor with thickness d_s , as shown on Fig. 1. We denote the bulk critical temperatures of the s -wave and s_{\pm} superconductors as T_c^s and T_c , respectively. The $x=0$ plane coincides with the interface between the superconductors. The main assumption of our description is that both superconductors are in dirty limit but the interband scattering in the s_{\pm} superconductor is negligible. In this case bulk superconductivity is described by quasiclassical Usadel equations²⁸ with boundary conditions derived in Ref. 29. The conventional proximity effects were extensively explored within this approach in Ref. 30. This description was later generalized to conventional two-band superconductors in Ref. 31. This model have been already used to describe some anomalous properties of the s/s_{\pm} interface in Refs. 22.

Both superconductors are described by the gap parameters, $\Delta(x)$, and the impurity averaged Green’s functions, which have regular and anomalous components, $G(x, \omega)$ and $F(x, \omega)$, with $G^2 + |F|^2 = 1$, where $\omega = 2\pi T(n+1/2)$ are the Matsubara frequencies. In the following, we will use subscript “s” for the s -wave superconductor and subscript “ α ” for the α -band of the s_{\pm} superconductor and skip subscripts in relations applicable for both superconductors. Further, we employ so-called Φ -parametrization^{30,31} in which the function $\Phi = \omega F/G$ is used instead of F . In this case $G = \omega/\sqrt{\omega^2 + |\Phi|^2}$. For the s -wave superconductor ($-d_s < x < 0$), the equations for the Green’s functions G_s and Φ_s and the self-

consistency equation are:

$$\frac{D_s}{2\omega G_s} \frac{d}{dx} \left[G_s^2 \frac{d\Phi_s}{dx} \right] - \Phi_s = -\Delta_s, \quad (4a)$$

$$2\pi T \sum_{\omega>0} \left(\frac{\Phi_s}{\sqrt{\omega^2 + |\Phi_s|^2}} - \frac{\Delta_s}{\omega} \right) + \Delta_s \ln \frac{T_c^s}{T} = 0 \quad (4b)$$

Correspondingly, for the s_{\pm} -superconductor, $0 < x < d_{\pm}$ we have

$$\frac{D_{\alpha}}{2\omega G_{\alpha}} \frac{d}{dx} \left[G_{\alpha}^2 \frac{d\Phi_{\alpha}}{dx} \right] - \Phi_{\alpha} = -\Delta_{\alpha}, \quad (5a)$$

$$2\pi T \sum_{\beta, \omega>0} \lambda_{\alpha\beta} \frac{\Phi_{\beta}}{\sqrt{\omega^2 + |\Phi_{\beta}|^2}} = \Delta_{\alpha}. \quad (5b)$$

where $\lambda_{\alpha\beta}$ is the coupling-constants matrix and α, β are the band indices. In Eq. (5a) we neglected the interband impurity scattering. For the case of s_{\pm} superconductor we consider here $\Delta_1 \Delta_2 < 0$. This is realized when $\lambda_{12}, \lambda_{21} < 0$. The diffusion coefficients $D_{\{s, \alpha\}}$ are related to the conductivities $\sigma_{\{s, \alpha\}}$ as $\sigma_{\{s, \alpha\}} = e^2 \nu_{\{s, \alpha\}} D_{\{s, \alpha\}}$, where $\nu_{\{s, \alpha\}}$ are the normal densities of states (DoS). The ratio of the off-diagonal coupling constants is given by the ratio of partial normal DoSs, $\lambda_{\alpha\beta}/\lambda_{\beta\alpha} = \nu_{\beta}/\nu_{\alpha}$. It is convenient to normalize all energy parameters (ω and gaps on *both* sides) to the same scale πT_c . We also introduce the coherence lengths $\xi_{\alpha} = \sqrt{D_{\alpha}/2\pi T_c}$ and $\xi_s^* = \sqrt{D_s/2\pi T_c}$ (note that ξ_s^* is related to the bulk coherence length of the s -wave superconductor by $\xi_s = \xi_s^* \sqrt{T_c/T_c^s}$).

The bulk equations have to be supplemented with the boundary conditions at the interface separating two superconductors. These conditions relate the Green’s functions and their derivatives at the interface and can be written as^{29,31}

$$\xi_s^* G_s \frac{d\Phi_s}{dx} = \sum_{\alpha} \frac{G_{\alpha}}{\tilde{\gamma}_{B\alpha}} (\Phi_{\alpha} - \Phi_s), \quad (6a)$$

$$\xi_{\alpha} G_{\alpha} \frac{d\Phi_{\alpha}}{dx} = -\frac{G_s}{\gamma_{B\alpha}} (\Phi_s - \Phi_{\alpha}), \quad (6b)$$

for $x=0$, where α is the band index. Here the coupling parameters, $\tilde{\gamma}_{B\alpha}$ and $\gamma_{B\alpha}$ are proportional to the partial boundary resistances $R_{B\alpha}$,

$$\tilde{\gamma}_{B\alpha} = \frac{R_{B\alpha}}{\rho_s \xi_s^*}, \quad \gamma_{B\alpha} = \frac{R_{B\alpha}}{\rho_{\alpha} \xi_{\alpha}}, \quad (7)$$

where $\rho_{\{s, \alpha\}} = 1/\sigma_{\{s, \alpha\}}$ are the bulk resistivities. We will also use the ratios of these parameters

$$\gamma_{\alpha} = \frac{\tilde{\gamma}_{B\alpha}}{\gamma_{B\alpha}} = \frac{\rho_{\alpha} \xi_{\alpha}}{\rho_s \xi_s^*}, \quad (8)$$

that are bulk parameters characterizing the relative “metallicity” of the s -wave superconductor and α band. In particular, large γ_{α} implies that the s -wave material is more metallic than the α band on the s_{\pm} side. The

parameters γ_α , $\lambda_{\alpha\beta}$, and ξ_α are not fully independent, the ratio of γ_α obeys the following relation

$$\frac{\gamma_1}{\gamma_2} = \frac{\nu_2 \xi_2}{\nu_1 \xi_1} = \frac{\lambda_{12} \xi_2}{\lambda_{21} \xi_1}. \quad (9)$$

The conditions at the external boundaries are $\Phi'_s(-d_s) = 0$ and $\Phi'_\alpha(d_\pm) = 0$.

The supercurrent flowing through the interface between the s-wave superconductor and α band is determined by the Green's functions $\Phi_{\{s,\alpha\}}$ at the interface as

$$j_\alpha = \frac{\mathcal{A}_0}{\tilde{\gamma}_{B\alpha}} 2\pi T \sum_{\omega>0} \frac{\text{Im}[\Phi_s^* \Phi_\alpha]}{\sqrt{\omega^2 + |\Phi_s|^2} \sqrt{\omega^2 + |\Phi_\alpha|^2}} \quad (10)$$

with $\mathcal{A}_0 = 1/(\epsilon\rho_s \xi_s^*)$. Substitution of the zero-order approximation for the Green's functions, $\Phi_{\{s,\alpha\}} \approx \Delta_{\{s,\alpha\}0}$, gives the well-known Ambegaokar-Baratoff result³² for the partial Josephson currents proportional to $\sin\phi$ with different signs corresponding to the signs of $\Delta_{\alpha 0}$. Here and below we assume for definiteness that ϕ is the phase shift between Δ_{s0} and Δ_{10} . To find the $\sin(2\phi)$ term in the Josephson current one has to go beyond the zero-order approximation and evaluate corrections to the Green's functions due to the interface. We discuss these corrections in the next section.

IV. PROXIMITY CORRECTIONS IN THE WEAK-COUPPLING LIMIT

In the case of weak coupling between the s and s_\pm superconductors, $\gamma_{B\alpha} \gg 1$, the contact-induced corrections to the gaps and Green's function can be treated as small perturbations, $\Delta_{\{s,\alpha\}}(x) = \Delta_{\{s,\alpha\}0} + \tilde{\Delta}_{\{s,\alpha\}}(x)$, $\Phi_{\{s,\alpha\}}(x) = \Delta_{\{s,\alpha\}0} + \tilde{\Phi}_{\{s,\alpha\}}(x)$. As a zero-order approximation, we consider a general complex case with a finite phase difference ϕ between the bulk gap parameters Δ_{10} and Δ_{s0} , see Fig. 2. For the *aligned* states such perturbative calculation has been reported in Ref. 22. Without loss of generality, we assume Δ_{s0} to be real. The small corrections $\tilde{\Phi}_{\{s,\alpha\}}(\omega, x)$ and $\tilde{\Delta}_{\{s,\alpha\}}(x)$ can be computed analytically in the linear order with respect to $1/\gamma_{B\alpha}$. Similar calculation for several types of junctions using somewhat different approach has been done in Ref. 33. The details of these derivations are described in Appendix A. In the TRSB state the solution for corrections exists only if the partial Josephson energies in the linear approximation exactly compensate each other, $E_{J1} = E_{J2}$. Here $E_{J\alpha}$ are related to the gaps and bound-

ary resistance $R_{B\alpha}$ by the standard expression

$$E_{J,\alpha} = \frac{\hbar}{2e^2 R_{B\alpha}} 2\pi T \sum_{\omega>0} \frac{\Delta_{s0} |\Delta_{\alpha 0}|}{\sqrt{\omega^2 + \Delta_{s0}^2} \sqrt{\omega^2 + |\Delta_{\alpha 0}|^2}}. \quad (11)$$

This also means that the total Josephson current flowing through the boundary is always zero in the ground state. The corrections can be presented in the form of Fourier

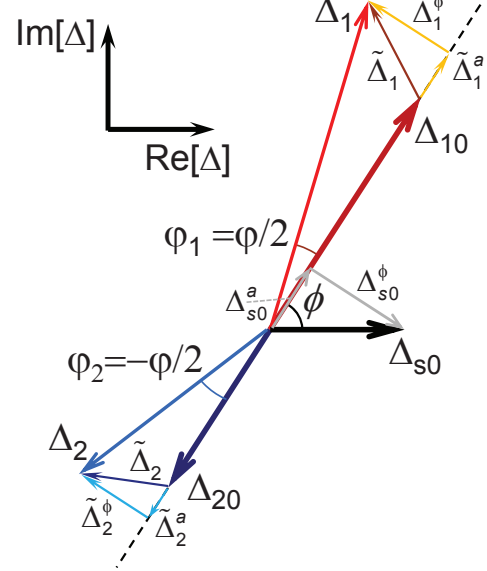


FIG. 2. Illustration of the bulk gap parameters, Δ_{s0} and $\Delta_{\alpha 0}$, and interface-induced corrections to the average s_\pm gaps, $\tilde{\Delta}_\alpha$, for a general TRSB state. The gap parameters are presented as vectors in the complex plane. Decompositions of Δ_{s0} and $\tilde{\Delta}_\alpha$ into the amplitude and phase components are also illustrated.

expansions. For the s -wave superconductor $\tilde{\Phi}_s(\omega, x) = \sum_{m=0}^{\infty} \tilde{\Phi}_{s,m}(\omega) \cos k_m x$, $\tilde{\Delta}_s(x) = \sum_{m=0}^{\infty} \tilde{\Delta}_{s,m} \cos k_m x$ with $k_m = m\pi/d_s$. The Fourier components of the Green's functions computed in Appendix A 1 are given by

$$\tilde{\Phi}_{s,m} = \frac{\tilde{\Delta}_{s,m}}{1 + \xi_{s,\omega}^2 k_m^2} + \frac{(2 - \delta_m) \xi_{s,\omega}^2 \xi_s^* / (d_s \xi_s^*)}{1 + \xi_{s,\omega}^2 k_m^2} \times \sum_{\alpha} \frac{\sqrt{\omega^2 + \Delta_{s0}^2}}{\sqrt{\omega^2 + |\Delta_{\alpha 0}|^2}} \frac{\Delta_{\alpha 0} - \Delta_{s0}}{\tilde{\gamma}_{B\alpha}}, \quad (12)$$

where $\xi_{s,\omega}^2 = \xi_{s,\Delta}^2 \Delta_{s0} / \sqrt{\omega^2 + \Delta_{s0}^2}$, $\xi_{s,\Delta}^2 = D_s / (2\Delta_{s0})$, and $\delta_m = 1(0)$ for $m = 0(m > 0)$. Here the first (bosonic) term is induced by the correction to the gap parameter and the second (fermionic) term is the direct response to the boundary perturbation. In the complex state the responses of the gap parameter are different in the amplitude and phase channels. As Δ_{s0} is selected real, these channels correspond to the real and imaginary parts of the gap correction, $\tilde{\Delta}_s = \tilde{\Delta}_s^R + i\tilde{\Delta}_s^I$. The Fourier components of $\tilde{\Delta}_s^R$ and $\tilde{\Delta}_s^I$ computed in Appendix A 1 can be presented as

$$\tilde{\Delta}_{s,m}^R = \frac{2\pi T}{Z_{s,m}^a} \sum_{\alpha,\omega>0} \frac{\omega^2}{(\omega^2 + \Delta_{s0}^2) \sqrt{\omega^2 + |\Delta_{\alpha 0}|^2}} \frac{(2 - \delta_m) \xi_{s,\Delta}^2 / (d_s \xi_s^*)}{\sqrt{\omega^2 + \Delta_{s0}^2 / \Delta_{s0} + (\pi m \xi_{s,\Delta} / d_s)^2}} \frac{\text{Re}[\Delta_{\alpha 0}] - \Delta_{s0}}{\tilde{\gamma}_{B\alpha}}, \quad (13a)$$

$$\text{with } Z_{s,m}^a = 2\pi T \sum_{\omega>0} \frac{1}{(\omega^2 + \Delta_{s0}^2)^{3/2}} \left(\Delta_{s0}^2 + \frac{\omega^2 (\pi m \xi_{s,\Delta} / d_s)^2}{\sqrt{\omega^2 + \Delta_{s0}^2 / \Delta_{s0} + (\pi m \xi_{s,\Delta} / d_s)^2}} \right)$$

$$\tilde{\Delta}_{s,m}^I = \frac{2\pi T}{Z_{s,m}^\phi} \sum_{\alpha,\omega>0} \frac{2\xi_{s,\Delta}^2 / (d_s \xi_s)}{\sqrt{\omega^2 + \Delta_{s0}^2 / \Delta_{s0} + (\pi m \xi_{s,\Delta} / d_s)^2}} \frac{1}{\sqrt{\omega^2 + |\Delta_{\alpha 0}|^2}} \frac{\text{Im}[\Delta_{\alpha 0}]}{\tilde{\gamma}_{B\alpha}}, \quad (13b)$$

$$\text{with } Z_{s,m}^\phi = 2\pi T \sum_{\omega>0} \frac{1}{\sqrt{\omega^2 + \Delta_{s0}^2}} \frac{(\pi m \xi_{s,\Delta} / d_s)^2}{\sqrt{\omega^2 + \Delta_{s0}^2 / \Delta_{s0} + (\pi m \xi_{s,\Delta} / d_s)^2}}.$$

For the s_\pm superconductor the corresponding Fourier series are $\tilde{\Phi}_\alpha = \sum_{m=0}^{\infty} \tilde{\Phi}_{\alpha,m} \cos q_m x$, $\tilde{\Delta}_\alpha = \sum_{m=0}^{\infty} \tilde{\Delta}_{\alpha,m} \cos q_m x$ with $q_m = m\pi/d_\pm$. Detailed derivations of the Fourier components are presented in Appendix A 2 and the result for $\tilde{\Phi}_{\alpha,m}$ can be written as,

$$\tilde{\Phi}_{\alpha,m} = \frac{\tilde{\Delta}_{\alpha,m}}{1 + \xi_{\alpha,\omega}^2 q_m^2} + \tilde{\Phi}_{\alpha,b,m}. \quad (14)$$

where

$$\xi_{\alpha,\omega}^2 = \xi_{\alpha,\Delta}^2 |\Delta_{\alpha 0}| / \sqrt{\omega^2 + |\Delta_{\alpha 0}|^2}, \quad \xi_{\alpha,\Delta}^2 = D_\alpha / (2|\Delta_{\alpha 0}|).$$

Here, as in Eq. (12), the first term is induced by the correction to the gap parameter and the second term is directly induced by the interface. For a general complex state, the corrections have to be split into the amplitude (along $\Delta_{\alpha 0}$) and phase channels, $\tilde{\Phi}_{\alpha,b,m} = \tilde{\Phi}_{\alpha,b,m}^a + \tilde{\Phi}_{\alpha,b,m}^\phi$, with

$$\begin{aligned} \begin{pmatrix} \tilde{\Phi}_{\alpha,b,m}^a \\ \tilde{\Phi}_{\alpha,b,m}^\phi \end{pmatrix} &= \frac{(2 - \delta_m) \xi_{\alpha,\omega}^2 / (d_\pm \xi_\alpha)}{\gamma_{B\alpha} (1 + \xi_{\alpha,\omega}^2 q_m^2)} \\ &\times \frac{\sqrt{\omega^2 + |\Delta_{\alpha 0}|^2}}{\sqrt{\omega^2 + \Delta_{s0}^2}} \begin{pmatrix} \Delta_{s0}^a - \Delta_{\alpha 0} \\ \Delta_{s0}^\phi \end{pmatrix}, \end{aligned} \quad (15)$$

where Δ_{s0}^a (Δ_{s0}^ϕ) is the projection of Δ_{s0} along $\Delta_{\alpha 0}$ (into perpendicular direction), as illustrated in Fig. 2. The gap corrections $\tilde{\Delta}_{\alpha,m}^{a,\phi}$ are related to $\tilde{\Phi}_{\alpha,b,m}^{a,\phi}$ as

$$\tilde{\Delta}_{\alpha,m}^a = 2\pi T \sum_{\beta,\omega>0} U_{m,\alpha\beta}^a \frac{\omega^2 \tilde{\Phi}_{\beta,b,m}^a}{(\omega^2 + |\Delta_{\beta 0}|^2)^{3/2}}, \quad (16a)$$

$$\tilde{\Delta}_{\alpha,m}^\phi = 2\pi T \sum_{\beta,\omega>0} U_{m,\alpha\beta}^\phi \frac{\tilde{\Phi}_{\beta,b,m}^\phi}{\sqrt{\omega^2 + |\Delta_{\beta 0}|^2}}, \quad (16b)$$

with the matrices $U_{m,\alpha\beta}^{a,\phi} = [w_{\alpha\beta} - \Sigma_{\alpha,m}^{a,\phi} \delta_{\alpha\beta}]^{-1}$ where

$$\begin{aligned} \Sigma_{\alpha,m}^a &= 2\pi T \sum_{\omega>0} \left[\frac{\omega^2}{(\omega^2 + |\Delta_{\alpha 0}|^2)^{3/2} (1 + \xi_{\alpha,\omega}^2 q_m^2)} - \frac{1}{\omega} \right] \\ &\quad + \ln \frac{T_c}{T}, \\ \Sigma_{\alpha,m}^\phi &= 2\pi T \sum_{\omega>0} \left[\frac{1}{\sqrt{\omega^2 + |\Delta_{\alpha 0}|^2} (1 + \xi_{\alpha,\omega}^2 q_m^2)} - \frac{1}{\omega} \right] \\ &\quad + \ln \frac{T_c}{T}, \end{aligned}$$

$w_{\alpha\beta} = \lambda_{\alpha\beta}^{-1} - \lambda^{-1} \delta_{\alpha\beta}$ and λ is the largest eigenvalue of the matrix $\lambda_{\alpha\beta}$. In the two-band case the explicit formulas for $w_{\alpha\beta}$ and $U_{m,\alpha\beta}^{a,\phi}$ are given in the Appendix A 2, Eqs. (A19) and (A27).

In summary, Eqs. (12) and (13) give corrections to the gap parameters and Green's function for the s -wave superconductor while Eqs. (14), (15), and (16) give corresponding results for the s_\pm superconductor. These corrections will allow us to derive in the next section a general result for the second harmonic of the Josephson current that determines the width of the TRSB region.

V. SECOND HARMONIC OF THE JOSEPHSON CURRENT

We already mentioned that the linear order with respect to the coupling strength $\propto 1/\tilde{\gamma}_{B\alpha}$ is not sufficient to determine the range of parameters where the TRSB state is realized. As discussed in Sec. II, in the weak-coupling regime this range is determined by the term $\propto \sin(2\phi)$ in the Josephson current that appears only in the quadratic order. In this section we derive microscopic expression for this term using corrections to the Green's functions presented in the previous section.

For arbitrary coupling the current density flowing through the interface between the s -wave superconduc-

tor and α -band is given by Eq. (10) and in ground state

$$j = \sum_{\alpha} j_{\alpha} = \mathcal{A}_0 \mathcal{I} = 0.$$

Here the parameter \mathcal{I} has dimensionality of energy. To find the second-order term in j , we have to expand the right hand side of Eq. (10) with respect to small corrections to Φ_s and Φ_{α} . This gives $\mathcal{I} \approx \mathcal{I}^{(1)} + \mathcal{I}^{(2)}$ where the

$$\mathcal{I}^{(2)} = 2\pi T \sum_{\alpha, \omega > 0} \frac{\text{Im}[\tilde{\Phi}_s^* \Delta_{\alpha 0} + \Delta_{s 0}^* \tilde{\Phi}_{\alpha}] - \text{Im}[\Delta_{s 0}^* \Delta_{\alpha 0}] \left(\frac{\text{Re}[\Delta_{s 0}^* \tilde{\Phi}_s]}{\omega^2 + |\Delta_{s 0}|^2} + \frac{\text{Re}[\Delta_{\alpha 0}^* \tilde{\Phi}_{\alpha}]}{\omega^2 + |\Delta_{\alpha 0}|^2} \right)}{\tilde{\gamma}_{B\alpha} \sqrt{\omega^2 + |\Delta_{\alpha 0}|^2} \sqrt{\omega^2 + |\Delta_{s 0}|^2}} \quad (19)$$

is the second-order term which is determined by the linear corrections to the Green's functions due to the interface perturbations, $\tilde{\Phi}_{\{s, \alpha\}}$, considered in the previous section. Using these results, we can present the corrections at $x = 0$ in the form

$$\tilde{\Phi}_s^R(0) = \sum_{\alpha} \mathcal{F}_{s, \alpha}^a \frac{\Delta_{s 0} + (-1)^{\alpha} |\Delta_{\alpha 0}| \cos \phi}{\tilde{\gamma}_{B\alpha}}, \quad (20a)$$

$$\tilde{\Phi}_s^I(0) = \sum_{\alpha} \mathcal{F}_{s, \alpha}^{\phi} \frac{(-1)^{\alpha} |\Delta_{\alpha 0}| \sin \phi}{\tilde{\gamma}_{B\alpha}} \quad (20b)$$

$$\tilde{\Phi}_{\alpha}^a(0) = \sum_{\beta} \mathcal{F}_{\alpha, \beta}^a \frac{\Delta_{s 0} - \Delta_{\beta 0}}{\gamma_{B\beta}}, \quad \tilde{\Phi}_{\alpha}^{\phi}(0) = \sum_{\beta} \mathcal{F}_{\alpha, \beta}^{\phi} \frac{\Delta_{s 0}^{\phi}}{\gamma_{B\beta}}, \quad (20c)$$

where the response functions of the s -wave superconductor in the amplitude and phase channels, $\mathcal{F}_{s, \alpha}^{a, \phi}(\omega)$, can be explicitly written as

$$\mathcal{F}_{s, \alpha}^a = -\frac{\xi_{s, \omega} / \xi_s^*}{\tanh(d_s / \xi_{s, \omega})} \frac{\sqrt{\omega^2 + \Delta_{s 0}^2}}{\sqrt{\omega^2 + |\Delta_{\alpha 0}|^2}} - \sum_{m=0}^{\infty} \frac{2 - \delta_m}{1 + \xi_{s, \omega}^2 k_m^2} \times \frac{2\pi T}{Z_{s, m}^a} \sum_{\omega_1 > 0} \frac{\omega_1^2}{(\omega_1^2 + \Delta_{s 0}^2) \sqrt{\omega_1^2 + |\Delta_{\alpha 0}|^2}} \frac{\xi_{s, \omega_1}^2 / (d_s \xi_s^*)}{1 + \xi_{s, \omega_1}^2 k_m^2}, \quad (21a)$$

$$\mathcal{F}_{s, \alpha}^{\phi} = -\frac{\xi_{s, \omega} / \xi_s^*}{\tanh(d_s / \xi_{s, \omega})} \frac{\sqrt{\omega^2 + \Delta_{s 0}^2}}{\sqrt{\omega^2 + |\Delta_{\alpha 0}|^2}} - \sum_{m=1}^{\infty} \frac{2}{1 + \xi_{s, \omega}^2 k_m^2} \times \frac{2\pi T}{Z_{s, m}^{\phi}} \sum_{\omega_1 > 0} \frac{1}{\sqrt{\omega_1^2 + |\Delta_{\alpha 0}|^2}} \frac{\xi_{s, \omega_1}^2 / (d_s \xi_s^*)}{1 + \xi_{s, \omega_1}^2 k_m^2}, \quad (21b)$$

with $Z_{s, m}^{a, \phi}$ defined in Eq. (13). The response functions of

term

$$\mathcal{I}^{(1)} = 2\pi T \sum_{\alpha, \omega > 0} \frac{\text{Im}[\Delta_{s 0}^* \Delta_{\alpha 0}]}{\tilde{\gamma}_{B\alpha} \sqrt{\omega^2 + |\Delta_{\alpha 0}|^2} \sqrt{\omega^2 + |\Delta_{s 0}|^2}} \quad (18)$$

corresponds to the standard main-order Josephson current and

the s_{\pm} superconductor, $\mathcal{F}_{\alpha, \beta}^{a, \phi}(\omega)$, are given by

$$\mathcal{F}_{\alpha, \beta}^a = \frac{\xi_{\alpha, \omega} / \xi_{\alpha}}{\tanh(d_{\pm} / \xi_{\alpha, \omega})} \frac{\sqrt{\omega^2 + |\Delta_{\alpha 0}|^2}}{\sqrt{\omega^2 + \Delta_{s 0}^2}} \delta_{\alpha\beta} + \sum_{m=0}^{\infty} \frac{2 - \delta_m}{1 + \xi_{\alpha, \omega}^2 q_m^2} \times 2\pi T \sum_{\omega_1 > 0} U_{m, \alpha\beta}^a \frac{\omega_1^2}{(\omega_1^2 + |\Delta_{\beta 0}|^2) \sqrt{\omega_1^2 + \Delta_{s 0}^2}} \frac{\xi_{\beta, \omega_1}^2 / (d_{\pm} \xi_{\beta})}{1 + \xi_{\beta, \omega_1}^2 q_m^2}, \quad (22a)$$

$$\mathcal{F}_{\alpha, \beta}^{\phi} = \mathcal{F}_{\alpha, 0}^{\phi} \delta_{\alpha\beta} + \frac{\xi_{\alpha, \omega} / \xi_{\alpha}}{\tanh(d_{\pm} / \xi_{\alpha, \omega})} \frac{\sqrt{\omega^2 + |\Delta_{\alpha 0}|^2}}{\sqrt{\omega^2 + \Delta_{s 0}^2}} \delta_{\alpha\beta} + \sum_{m=1}^{\infty} \frac{2}{1 + \xi_{\alpha, \omega}^2 q_m^2} 2\pi T \sum_{\omega_1 > 0} U_{m, \alpha\beta}^{\phi} \frac{1}{\sqrt{\omega_1^2 + \Delta_{s 0}^2}} \frac{\xi_{\beta, \omega_1}^2 / (d_{\pm} \xi_{\beta})}{1 + \xi_{\beta, \omega_1}^2 q_m^2}, \quad (22b)$$

where the matrices $U_{m, \alpha\beta}^{a, \phi}$ are defined in Eq. (A27), and the term

$$\mathcal{F}_{\alpha, 0}^{\phi} = \frac{2\pi T}{2d_{\pm} w_{12} |\Delta_{20}|} \sum_{\omega > 0} \frac{\xi_{1, \omega} / \xi_1}{\sqrt{\omega^2 + \Delta_{s 0}^2}} |\Delta_{\alpha 0}| \quad (23)$$

describes the contribution from the uniform phase corrections $\tilde{\Delta}_{\alpha, 0}^{\phi}$ given by Eq. (A29). The different quantities entering Eq. (19) can now be expressed as

$$\begin{aligned} \text{Im}[\Delta_{s 0}^* \Delta_{\alpha 0}] &= -\Delta_{s 0} |\Delta_{\alpha 0}| (-1)^{\alpha} \sin \phi, \\ \text{Im}[\tilde{\Phi}_s^* \Delta_{\alpha 0}] &= |\Delta_{\alpha 0}| \sum_{\beta} \frac{1}{\tilde{\gamma}_{B\beta}} [-\mathcal{F}_{s, \beta}^a \Delta_{s 0} (-1)^{\alpha} \sin \phi \\ &\quad - (\mathcal{F}_{s, \beta}^a - \mathcal{F}_{s, \beta}^{\phi}) |\Delta_{\beta 0}| (-1)^{\alpha + \beta} \sin \phi \cos \phi], \\ \text{Im}[\Delta_{s 0}^* \tilde{\Phi}_{\alpha}] &= \Delta_{s 0} \sum_{\beta} \frac{1}{\gamma_{B\beta}} [(-1)^{\beta} \mathcal{F}_{\alpha, \beta}^a |\Delta_{\beta 0}| \sin \phi \\ &\quad + (\mathcal{F}_{\alpha, \beta}^a - \mathcal{F}_{\alpha, \beta}^{\phi}) \Delta_{s 0} \sin \phi \cos \phi], \\ \text{Re}[\Delta_{s 0}^* \tilde{\Phi}_s^a] &= \Delta_s \sum_{\beta} \mathcal{F}_{s, \beta}^a \frac{\Delta_{s 0} + (-1)^{\beta} |\Delta_{\beta 0}| \cos \phi}{\tilde{\gamma}_{B\beta}}, \\ \text{Re}[\Delta_{\alpha 0}^* \tilde{\Phi}_{\alpha}] &= -(-1)^{\alpha} |\Delta_{\alpha 0}| \sum_{\beta} \mathcal{F}_{\alpha, \beta}^a \frac{\Delta_{s 0} \cos \phi + (-1)^{\beta} |\Delta_{\beta 0}|}{\gamma_{B\beta}}. \end{aligned}$$

We can see that $\mathcal{I}^{(2)}$ contains terms proportional to $\sin \phi$ and $\sin \phi \cos \phi = \frac{1}{2} \sin(2\phi)$, $\mathcal{I}^{(2)} = \mathcal{J}^{(1)} \sin \phi + \mathcal{J}^{(2)} \cos \phi \sin \phi$. The terms $\propto \sin \phi$ just slightly shift location of the transition line. The transition order and possible width of the TRSB region are determined by the terms $\propto \sin \phi \cos \phi$. Collecting such terms in \mathcal{I} , we obtain

$$\begin{aligned} \mathcal{J}^{(2)} &= 2\pi T \sum_{\alpha, \omega > 0} \frac{|\Delta_{\alpha 0}| \Delta_{s 0} \mathcal{R}_{\alpha}(\omega)}{\tilde{\gamma}_{B\alpha} \sqrt{\omega^2 + |\Delta_{\alpha 0}|^2} \sqrt{\omega^2 + \Delta_{s 0}^2}} \quad (24) \\ \mathcal{R}_{\alpha}(\omega) &= \sum_{\beta} \left[-\frac{|\Delta_{\beta 0}| (-1)^{\alpha+\beta}}{\tilde{\gamma}_{B\beta} \Delta_{s 0}} \left(\frac{\omega^2 \mathcal{F}_{s,\beta}^a}{\omega^2 + \Delta_{s 0}^2} - \mathcal{F}_{s,\beta}^{\phi} \right) \right. \\ &\quad \left. + \frac{\Delta_{s 0}}{\gamma_{B\beta} |\Delta_{\alpha 0}|} \left(\frac{\omega^2 \mathcal{F}_{\alpha\beta}^a}{\omega^2 + |\Delta_{\alpha 0}|^2} - \mathcal{F}_{\alpha\beta}^{\phi} \right) \right] \end{aligned}$$

The term corresponding to the uniform phase tilt $\mathcal{F}_{\alpha,0}^{\phi}$, Eq. (23) has special meaning and it is useful to evaluate it explicitly,

$$\begin{aligned} \mathcal{J}_{\phi,0}^{(2)} &= - \left(\frac{2\pi T}{\tilde{\gamma}_{B1}} \sum_{\omega > 0} \frac{\Delta_{s 0} |\Delta_{10}|}{\sqrt{\omega^2 + |\Delta_{10}|^2} \sqrt{\omega^2 + |\Delta_{s 0}|^2}} \right)^2 \\ &\quad \times \frac{\gamma_1 \xi_{1,\Delta}^2 |\Delta_{10}| / \xi_1}{d_{\pm} w_{12} |\Delta_{10}| |\Delta_{20}|} \\ &= - \frac{2e^2}{\hbar} E_{J,1}^2 \frac{\rho_s \xi_s}{d_{\pm} \nu_1 w_{12} |\Delta_{10}| |\Delta_{20}|}, \quad (25) \end{aligned}$$

where we used the relations $\gamma_1 \xi_{1,\Delta}^2 |\Delta_{10}| / \xi_1 = \hbar \rho_1 D_1 / (2\rho_s \xi_s) = \hbar / (2e^2 \nu_1 \rho_s \xi_s)$. This gives the following contribution to the second harmonic of the Josephson current

$$j_{\phi,0}^{(2)} = -j_{J,1} \frac{E_{J,1}}{2d_{\pm} \nu_1 w_{12} |\Delta_{10}| |\Delta_{20}|}. \quad (26)$$

The quantity $\mathcal{E}_{12} = d_{\pm} \nu_1 w_{12} |\Delta_{10}| |\Delta_{20}|$ in the denominator represents the interband coupling energy. Therefore this result exactly corresponds to the result of the frustrated Josephson junction model. This term, however, dominates only in the case of small interband coupling energy, when the parameter w_{12} is very small.

To gain a further insight on the structure of the second-harmonic amplitude $\mathcal{J}^{(2)}$, we present it explicitly as a sum of terms corresponding to contributions from the corrections to the s -wave and s_{\pm} Green's functions coming directly from the interface ($\mathcal{J}_{b,*}^{(2)}$) and via gap parameters ($\mathcal{J}_{\Delta,*}^{(2)}$).

$$\mathcal{J}^{(2)} = \mathcal{J}_{b,s}^{(2)} + \mathcal{J}_{\Delta,s}^{(2)} + \mathcal{J}_{b,\text{pm}}^{(2)} + \mathcal{J}_{\Delta,\text{pm}}^{(2)} + \mathcal{J}_{\phi,0}^{(2)} \quad (27)$$

We already considered above the last term, $\mathcal{J}_{\phi,0}^{(2)}$, that is part of $\mathcal{J}_{\Delta,\text{pm}}^{(2)}$ coming the uniform phase response of s_{\pm} superconductor. This term requires separate treatment leading to Eq. (25) which corresponds to the result of the frustrated Josephson junction model. As for the other terms, the s -wave components are given by the following explicit formulas,

$$\mathcal{J}_{b,s}^{(2)} = -2\pi T \sum_{\omega > 0} \left(\sum_{\alpha} \frac{\Delta_{\alpha 0}}{\tilde{\gamma}_{B\alpha} \sqrt{\omega^2 + |\Delta_{\alpha 0}|^2}} \right)^2 \frac{\Delta_{s 0}^2}{\omega^2 + \Delta_{s 0}^2} \frac{\xi_{s,\omega} / \xi_s}{\tanh(d_s / \xi_{s,\omega})}, \quad (28a)$$

$$\mathcal{J}_{\Delta,s}^{(2)} = -\frac{\xi_{s,\Delta}^2}{\Delta_{s 0} d_s \xi_s} \left[-\frac{Y_{a,0}^2}{Z_{s,0}^a} + 2 \sum_{m=1}^{\infty} \left(\frac{Y_{\phi,m}^2}{Z_{s,m}^{\phi}} - \frac{Y_{a,m}^2}{Z_{s,m}^a} \right) \right], \quad (28b)$$

$$Y_{\phi,m} = 2\pi T \sum_{m,\alpha,\omega > 0} \frac{\Delta_{\alpha 0}}{\tilde{\gamma}_{B\alpha} \sqrt{\omega^2 + |\Delta_{\alpha 0}|^2} \left(\sqrt{\omega^2 + \Delta_{s 0}^2} / \Delta_{s 0} + \xi_{\Delta,s}^2 k_m^2 \right)},$$

$$Y_{a,m} = 2\pi T \sum_{m,\alpha,\omega > 0} \frac{\Delta_{\alpha 0} \omega^2}{\tilde{\gamma}_{B\alpha} \sqrt{\omega^2 + |\Delta_{\alpha 0}|^2} (\omega^2 + \Delta_{s 0}^2) \left(\sqrt{\omega^2 + \Delta_{s 0}^2} / \Delta_{s 0} + \xi_{\Delta,s}^2 k_m^2 \right)},$$

while the s_{\pm} components can be written as

$$\mathcal{J}_{b,\text{pm}}^{(2)} = -2\pi T \sum_{\alpha, \omega > 0} \frac{1}{\tilde{\gamma}_{B\alpha} \gamma_{B\alpha}} \frac{\Delta_{s0}^2 |\Delta_{\alpha 0}|^2}{(\omega^2 + \Delta_{s0}^2)(\omega^2 + |\Delta_{\alpha 0}|^2)} \frac{\xi_{\alpha, \omega} / \xi_{\alpha}}{\tanh(d_{\pm} / \xi_{\alpha, \omega})}, \quad (29a)$$

$$\mathcal{J}_{\Delta, \text{pm}}^{(2)} = -\frac{\pi T_c}{d_{\pm}} \Delta_{s0}^2 \sum_{\alpha, \beta} \left[-X_{0, \alpha}^a U_{0, \alpha \beta}^a \gamma_{\beta} \xi_{\beta} X_{0, \beta}^a + 2 \sum_{m=1}^{\infty} \left(X_{m, \alpha}^{\phi} U_{m, \alpha \beta}^{\phi} \gamma_{\beta} \xi_{\beta} X_{m, \beta}^{\phi} - X_{m, \alpha}^a U_{m, \alpha \beta}^a \gamma_{\beta} \xi_{\beta} X_{m, \alpha}^a \right) \right], \quad (29b)$$

$$X_{m, \alpha}^{\phi} = \frac{2\pi T}{\tilde{\gamma}_{B\alpha}} \sum_{\omega > 0} \frac{1}{\sqrt{\omega^2 + \Delta_{s0}^2} \left(\sqrt{\omega^2 + |\Delta_{\alpha 0}|^2} + |\Delta_{\alpha 0}| \xi_{\Delta, \alpha}^2 q_m^2 \right)},$$

$$X_{m, \alpha}^a = \frac{2\pi T}{\tilde{\gamma}_{B\alpha}} \sum_{\omega > 0} \frac{\omega^2}{\sqrt{\omega^2 + \Delta_{s0}^2} (\omega^2 + |\Delta_{\alpha 0}|^2) \left(\sqrt{\omega^2 + |\Delta_{\alpha 0}|^2} + |\Delta_{\alpha 0}| \xi_{\Delta, \alpha}^2 q_m^2 \right)}.$$

We note also a useful relation for the combination $\gamma_{\beta} \xi_{\beta}$ entering Eq. (29b), $\gamma_{\beta} \xi_{\beta} = \xi_s^* \nu_s / \nu_{\beta}$. In summary, Eqs. (25), (28), and (29) give general expressions for the components contributing to the second harmonic of Josephson current in Eq. (27). Even though these formulas are rather cumbersome, they are suitable for numerical evaluation of the second-harmonic amplitude for arbitrary parameters of superconductors and interface. In the next section we analyze these terms for practically important particular case in which much simpler analytical results can be derived.

A. Analysis of terms for low temperatures in the case $d_s < \xi_s$ and $\Delta_s \ll |\Delta_{\alpha}|$

Unfortunately, general formulas derived in the previous section are rather cumbersome. To understand better the relation between different terms and their absolute values, in this section we evaluate them at low temperature and for the most interesting case of weaker s -wave superconductor, small d_s and large d_{\pm} . In these limits it is possible to derive simple analytical results for the most important terms.

1. Terms $\mathcal{J}_{b,s}^{(2)}$ and $\mathcal{J}_{\Delta,s}^{(2)}$

For very thin s -wave superconductor the dominating in $1/d_s$ order term is coming from $\mathcal{J}_{b,s}^{(2)}$ and the $m=0$ term in the amplitude part of $\mathcal{J}_{\Delta,s}^{(2)}$ which we will notate as $\mathcal{J}_{\Delta,s,0}^{(2)}$,

$$\mathcal{J}_{b,s}^{(2)} = -\frac{1}{d_s} \int_0^{\infty} d\omega \left(\sum_{\alpha} \frac{\Delta_{\alpha 0}}{\tilde{\gamma}_{B\alpha} \sqrt{\omega^2 + |\Delta_{\alpha 0}|^2}} \right)^2 \frac{\Delta_{s0}^2}{(\omega^2 + \Delta_{s0}^2)^{3/2}},$$

$$\mathcal{J}_{\Delta,s,0}^{(2)} \approx \frac{1}{d_s} \left(\sum_{\alpha} \int_0^{\infty} d\omega \frac{\Delta_{\alpha 0} \Delta_{s0}^2}{\tilde{\gamma}_{B\alpha} \sqrt{\omega^2 + |\Delta_{\alpha 0}|^2} (\omega^2 + \Delta_{s0}^2)^{3/2}} \right)^2,$$

where in the last formula we used a compensation condition for the Josephson energy near the transition point. In the limit $\Delta_{s0} \ll |\Delta_{\alpha 0}|$ integrals converge at $\omega \sim \Delta_{s0}$ and one may think than it is possible to replace $\frac{|\Delta_{\alpha 0}|}{\sqrt{\omega^2 + |\Delta_{\alpha 0}|^2}} \rightarrow 1$ under the frequency integrals. However, as $\int_0^{\infty} d\omega \frac{\Delta_{s0}^2}{(\omega^2 + \Delta_{s0}^2)^{3/2}} = 1$, within this approximation the two terms in the sum

$$\mathcal{J}_{0,s}^{(2)} = \mathcal{J}_{b,s}^{(2)} + \mathcal{J}_{\Delta,s,0}^{(2)}$$

exactly compensate each other,

$$\left(\begin{array}{c} \mathcal{J}_{b,s}^{(2)} \\ \mathcal{J}_{\Delta,s,0}^{(2)} \end{array} \right) \approx \mp \frac{1}{d_s} \left(\sum_{\alpha} \frac{(-1)^{\alpha}}{\tilde{\gamma}_{B\alpha}} \right)^2,$$

and therefore they must be evaluated in higher order with respect to $\Delta_{s0}/|\Delta_{\alpha 0}|$. To proceed, we introduce the definitions

$$L(\omega) = \sum_{\alpha} \frac{(-1)^{\alpha} |\Delta_{\alpha 0}|}{\tilde{\gamma}_{B\alpha} \sqrt{\omega^2 + |\Delta_{\alpha 0}|^2}} = L_0 + L_1(\omega),$$

with $L_0 = \sum_{\alpha} (-1)^{\alpha} / \tilde{\gamma}_{B\alpha}$ and

$$L_1(\omega) = \sum_{\alpha} \frac{(-1)^{\alpha}}{\tilde{\gamma}_{B\alpha}} \left(\frac{|\Delta_{\alpha 0}|}{\sqrt{\omega^2 + |\Delta_{\alpha 0}|^2}} - 1 \right),$$

which allows us to represent

$$\mathcal{J}_{b,s}^{(2)} = -\frac{1}{d_s} \int_0^{\infty} d\omega L^2(\omega) \frac{\Delta_{s0}^2}{(\omega^2 + \Delta_{s0}^2)^{3/2}},$$

$$\mathcal{J}_{\Delta,s,0}^{(2)} = \frac{1}{d_s} \left(\int_0^{\infty} d\omega L(\omega) \frac{\Delta_{s0}^2}{(\omega^2 + \Delta_{s0}^2)^{3/2}} \right)^2,$$

and rewrite $\mathcal{J}_{0,s}^{(2)}$ as

$$\mathcal{J}_{0,s}^{(2)} = \frac{1}{d_s} \left(\int_0^{\infty} d\omega L_1(\omega) \frac{\Delta_s^2}{(\omega^2 + \Delta_s^2)^{3/2}} \right)^2 - \frac{1}{d_s} \int_0^{\infty} d\omega L_1^2(\omega) \frac{\Delta_s^2}{(\omega^2 + \Delta_s^2)^{3/2}}.$$

The dominating contribution is coming from the second term and evaluating integral, we finally obtain

$$\mathcal{J}_{0,s}^{(2)} \approx -\frac{\Delta_s^2}{d_s} \left[\frac{2 \ln 2 - 1}{2} \left(\sum_{\alpha} \frac{(-1)^{\alpha}}{\tilde{\gamma}_{B\alpha} |\Delta_{\alpha}|} \right)^2 - \frac{\frac{1}{|\Delta_1|^2} \ln \left(1 + \frac{|\Delta_1|}{|\Delta_2|} \right) + \frac{1}{|\Delta_2|^2} \ln \left(1 + \frac{|\Delta_2|}{|\Delta_1|} \right) - \frac{2 \ln 2}{|\Delta_1| |\Delta_2|}}{\tilde{\gamma}_{B1} \tilde{\gamma}_{B2}} \right] \quad (30)$$

It is interesting to note that this $1/d_s$ term only exists in the asymmetric case, it vanishes for identical s_{\pm} bands.

2. Term $\mathcal{J}_{b,\text{pm}}^{(2)}$

The term $\mathcal{J}_{b,\text{pm}}^{(2)}$ in Eq. (29a) for $T = 0$ and $d_{\pm} \gg \xi_{\alpha}$ becomes

$$\mathcal{J}_{b,\text{pm}}^{(2)} = -\sqrt{\pi T_c} \sum_{\alpha} \frac{\Delta_{s0}^2 |\Delta_{\alpha 0}|^2}{\tilde{\gamma}_{B\alpha} \gamma_{B\alpha}} \times \int_0^{\infty} \frac{d\omega}{(\omega^2 + \Delta_{s0}^2)(\omega^2 + |\Delta_{\alpha 0}|^2)^{5/4}}. \quad (31)$$

For $\Delta_{s0} \ll |\Delta_{\alpha 0}|$ we can evaluate the frequency integral leading to the quite simple result

$$\mathcal{J}_{b,\text{pm}}^{(2)} \approx -\frac{\pi}{2} \sum_{\alpha} \frac{\Delta_{s0}}{\tilde{\gamma}_{B\alpha} \gamma_{B\alpha}} \sqrt{\frac{\pi T_c}{|\Delta_{\alpha 0}|}}. \quad (32)$$

In most cases *this is actually a dominating term* which may be used for an approximate evaluation of the total second-harmonic amplitude. It has only linear order with respect to Δ_{s0} , while other terms are proportional to Δ_{s0}^2 . Also, for a typical contact $\gamma_{\alpha} = \tilde{\gamma}_{B\alpha} / \gamma_{B\alpha} \gg 1$ due to semimetallic nature of iron-based superconductors, which enhances $\mathcal{J}_{*,\text{pm}}^{(2)}$ terms in comparison with $\mathcal{J}_{*,s}^{(2)}$ terms. The negative sign of $\mathcal{J}_{b,\text{pm}}^{(2)}$ implies the continuous-transition scenario and the existence of the TRSB state. In particular, comparing $\mathcal{J}_{b,\text{pm}}^{(2)}$ with term $\mathcal{J}_{0,s}^{(2)}$, Eq. (30), we obtain, up to a dimensionless function of the ratios $\tilde{\gamma}_{B1} / \tilde{\gamma}_{B2}$ and $|\Delta_{10}| / |\Delta_{20}|$,

$$\frac{\mathcal{J}_{b,\text{pm}}^{(2)}}{\mathcal{J}_{0,s}^{(2)}} \approx \gamma_1 \frac{d_s}{\xi_s^*} \frac{|\Delta_{10}|}{\Delta_{s0}},$$

which means that the s -wave term $\mathcal{J}_{0,s}^{(2)}$ exceeds $\mathcal{J}_{b,\text{pm}}^{(2)}$ only for an extremely thin s -wave layer $d_s < \xi_s^* \Delta_{s0} / (\gamma_1 |\Delta_{10}|)$. Another factor further enhancing this ratio is that different s_{\pm} bands contribute to $\mathcal{J}_{b,\text{pm}}^{(2)}$ with the same sign while their contributions to $\mathcal{J}_{0,s}^{(2)}$ partially compensate one another.

3. Term $\mathcal{J}_{\Delta,\text{pm}}^{(2)}$

Finally, we obtain the limiting form for the most complicated term $\mathcal{J}_{\Delta,\text{pm}}^{(2)}$ in Eq. (29b). The quantities $\Sigma_{m,\alpha}^{a,\phi}$ that determine the matrices $U_{m,\alpha\beta}^{a,\phi}$ in Eq. (A27) can be evaluated at $T = 0$ exactly:

$$\Sigma_{m,\alpha}^{a,\phi} = g_{a,\phi}(a_m) - \ln \left(\frac{|\Delta_{\alpha 0}|}{4\pi T_c} \right) + \psi(1/2), \quad (33a)$$

$$g_{\phi}(a) = -\frac{2a}{\sqrt{1-a^2}} \arctan \sqrt{\frac{1-a}{1+a}}, \quad (33b)$$

$$g_a(a) = -\frac{2}{a} \left(\frac{\pi}{4} - \sqrt{1-a^2} \arctan \sqrt{\frac{1-a}{1+a}} \right), \quad (33c)$$

where $a_m = (\pi m \xi_{\alpha, \Delta} / d_{\pm})^2$ and $\psi(x)$ is the digamma function. The quantities $X_{m,\alpha}^{a,\phi}$ can be evaluated approximately in the limit $\Delta_{s0} \ll |\Delta_{\alpha 0}|$,

$$X_{m,\alpha}^{\phi} \approx \frac{1}{\tilde{\gamma}_{B\alpha} |\Delta_{\alpha 0}|} \frac{1}{1+a_m} \left(\ln \frac{4|\Delta_{\alpha 0}|}{\Delta_{s0}} + \frac{a_m}{1-a_m} \ln \frac{2}{1+a_m} \right), \quad (34a)$$

$$X_{m,\alpha}^a \approx \frac{1}{\tilde{\gamma}_{B\alpha} |\Delta_{\alpha 0}|} \frac{\ln(1+a_m)}{a_m}. \quad (34b)$$

Assuming that the values for ξ_{α} , $|\Delta_{\alpha 0}|$, and γ_{α} for different α are close, the term $\mathcal{J}_{\Delta,\text{pm}}^{(2)}$ can be roughly estimated as

$$\mathcal{J}_{\Delta,\text{pm}}^{(2)} \sim \pi T_c \frac{\Delta_{s0}^2}{\tilde{\gamma}_{B1} \gamma_{B1} \Delta_{10}^2} \quad (35)$$

and we can see that this term is typically smaller than $\mathcal{J}_{b,\text{pm}}^{(2)}$, Eq. (32), by the ratio $\Delta_{s0} / \Delta_{10}$ (assuming $\Delta_{10} / \pi T_c \sim 1$).

B. Region near T_c^s for $T_c^s \ll T_c$

Near the transition temperature of the s -wave superconductor all terms contributing to $\mathcal{J}^{(2)}$ decrease as Δ_{s0}^2 . In particular, the dominating term $\mathcal{J}_{b,\text{pm}}^{(2)}$ behaves as

$$\mathcal{J}_{b,\text{pm}}^{(2)} \approx -\frac{\pi}{4} \sum_{\alpha} \sqrt{\frac{\pi T_c}{|\Delta_{\alpha 0}|}} \frac{\Delta_{s0}^2 / T_c^s}{\tilde{\gamma}_{B\alpha} \gamma_{B\alpha}} \text{ for } T \rightarrow T_c^s - 0. \quad (36)$$

This behavior has an important consequence: the width of the TRSB state shrinks with increasing temperature. On the other hand, the weak coupling approach breaks down when the temperature is too close to T_c^s when the correction to the s -wave gap becomes comparable with its bulk value.

VI. WIDTH OF TRSB REGION

To analyze the width of the TRSB region in the weak-coupling regime, we represent the supercurrent flowing through the interface in the form $j = \sum_{\alpha} j_{\alpha} =$

$\mathcal{A}_0 (\mathcal{J}^{(1)} \sin \phi + \mathcal{J}^{(2)} \cos \phi \sin \phi)$. The transition roughly corresponds to the vanishing of the first harmonic $\mathcal{J}^{(1)}$ which we can represent as

$$\mathcal{J}^{(1)} = \sum_{\alpha} \frac{(-1)^{\alpha}}{\tilde{\gamma}_{B\alpha}} \Delta_{s0} f_{J,\alpha}, \quad (37)$$

with

$$\begin{aligned} f_{J,\alpha} &\equiv f_J \left(\frac{|\Delta_{\alpha 0}|}{T}, \frac{\Delta_{s0}}{T} \right) \\ &= 2\pi T \sum_{\omega > 0} \frac{|\Delta_{\alpha 0}|}{\sqrt{\omega^2 + |\Delta_{\alpha 0}|^2} \sqrt{\omega^2 + |\Delta_{s0}|^2}}. \end{aligned}$$

We remind that the TRSB state only exists if $\mathcal{J}^{(2)} < 0$. In this case, which is realized for our system, we can write the condition for the TRSB state range as

$$\left| \frac{f_{J,1}}{\tilde{\gamma}_{B1}} - \frac{f_{J,2}}{\tilde{\gamma}_{B2}} \right| < \frac{|\mathcal{J}^{(2)}|}{\Delta_{s0}}. \quad (38)$$

This formula together with microscopic results for $\mathcal{J}^{(2)}$ of the previous section represent the main results of this paper. For fixed $\tilde{\gamma}_{B1}^{-1}$ the transition from aligned to TRSB state occurs at the following values of $\tilde{\gamma}_{B2}^{-1}$

$$\frac{1}{\tilde{\gamma}_{B2}} = \frac{f_{J,1}}{f_{J,2} \tilde{\gamma}_{B1}} \pm \frac{\mathcal{J}^{(2)}}{\Delta_{s0} f_{J,2}}.$$

As $\mathcal{J}^{(2)}$ scales as $\tilde{\gamma}_{B\alpha}^{-2}$, The width of the TRSB region can be conveniently characterized by the parameter

$$\tilde{\gamma}_{B2}^2 \Delta \tilde{\gamma}_{B2}^{-1} \approx \Delta \tilde{\gamma}_{B2} = \frac{2\tilde{\gamma}_{B2}^2 \mathcal{J}^{(2)}}{\Delta_{s0} f_{J,2}}, \quad (39)$$

which depends only on bulk properties of the superconductors and does not depend on the boundary resistances.³⁴ In particular, at low temperatures and for $\Delta_{s0} \ll |\Delta_{20}|$, using the asymptotic $f_{J,\alpha} \approx \ln(4|\Delta_{\alpha 0}|/\Delta_{s0})$ and keeping only the dominating term in $\mathcal{J}^{(2)}$, Eq. (32), we obtain the following estimate

$$\Delta \tilde{\gamma}_{B2} \approx \pi \ln \frac{4|\Delta_{20}|}{\Delta_{s0}} \sum_{\alpha} \frac{\gamma_{\alpha}}{\left(\ln \frac{4|\Delta_{\alpha 0}|}{\Delta_{s0}} \right)^2} \sqrt{\frac{\pi T_c}{|\Delta_{\alpha 0}|}}. \quad (40)$$

We can see that this width only weakly depends on the value of the s -wave gap and is mostly determined by the parameters γ_{α} . Using the definition of $\tilde{\gamma}_{B\alpha}$ and γ_{α} , Eqs. (7) and (8), we immediately obtain a simple estimate for the spread of the partial boundary resistance ΔR_{B2} within which the TRSB state exists,

$$\Delta R_{B2} \approx \pi \ln \frac{4|\Delta_{20}|}{\Delta_{s0}} \sum_{\alpha} \frac{\rho_{\alpha} \xi_{\alpha}}{\left(\ln \frac{4|\Delta_{\alpha 0}|}{\Delta_{s0}} \right)^2} \sqrt{\frac{\pi T_c}{|\Delta_{\alpha 0}|}}, \quad (41)$$

which is mainly determined by the products $\rho_{\alpha} \xi_{\alpha}$.

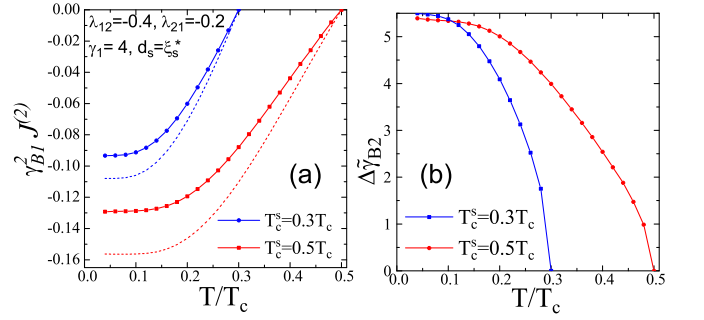


FIG. 3. (a) Temperature dependences of the second-harmonic amplitude for two values of the ratio T_c^s/T_c , 0.3 and 0.5. Dashed lines show the term $\mathcal{J}_{b,pm}^{(2)}$ only. Other parameters are shown in the plot. We also assume $\lambda_{11} = \lambda_{22} = 0$. (b) Corresponding temperature dependences of the TRSB width, Eq. (39).

Figure 3 illustrates the temperature dependences of the second-harmonic amplitude $\mathcal{J}^{(2)}$ and the width of the TRSB region for the representative parameters listed in the left figure and for the two values of the ratio T_c^s/T_c , 0.3 and 0.5. In Fig. 3(a) we show for comparison both the full amplitude of the second harmonic and the term $\mathcal{J}_{b,pm}^{(2)}$ only (dashed lines). We can see that this term typically accounts for 80% – 85% of the total amplitude. The remaining part mostly comes from the terms $\mathcal{J}_{\Delta,pm}^{(2)}$ and $\mathcal{J}_{\phi,0}^{(2)}$. For used representative parameters the contributions from the s -wave terms $\mathcal{J}_{*,s}^{(2)}$ are negligible. We emphasize the shrinking of the TRSB width illustrated in Fig. 3(b), $\Delta \tilde{\gamma}_{B2} \propto \sqrt{T_c^s - T}$ near T_c^s . This means that in some range of parameters, the transition from the aligned to TRSB state may be observed as a function of temperature, as in the case of the $0-\pi$ transition in SFS junctions.³⁵

VII. DENSITY OF STATES OF S-WAVE SUPERCONDUCTOR WITHIN THE TRSB REGION

Contact with s_{\pm} superconductor induces specific features in the s -wave density of states (DOS). For the *aligned* states in the case of thin s -wave layer, the s_{\pm} gaps aligned with Δ_{s0} generate positive corrections to DoS, while anti-aligned gaps generate negative corrections.²² The latter negative features can be used to identify s_{\pm} state.

In this short section we consider evolution of contact-induced features of the s -wave DoS across the TRSB region. To find the density of states, we have to perform analytical continuation of the Green's functions to real energies $i\omega \rightarrow E + i\delta$. The normalized DoS is related to the real-energy Green's function by the standard expres-

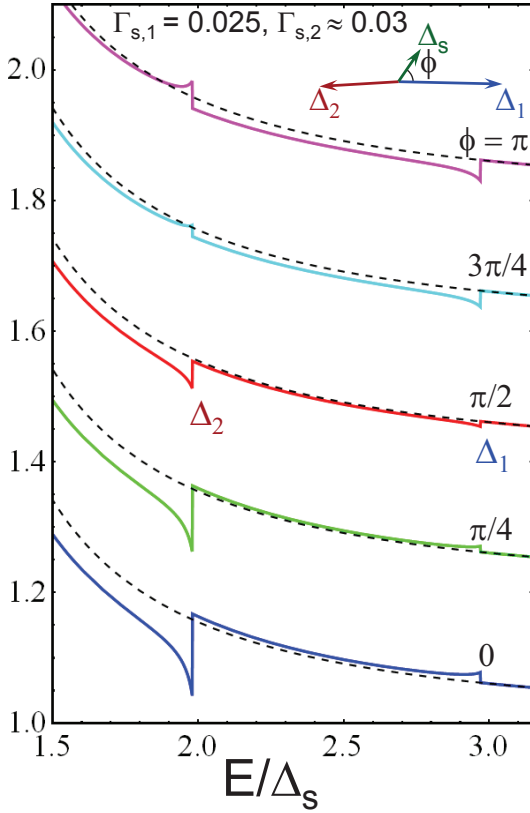


FIG. 4. Evolution of the proximity-induced features in the s -wave DoS within the TRSB region with increasing angle ϕ between Δ_{s0} and Δ_{10} . Curves are vertically displaced for clarity. Dashed lines show the bulk DoS.

sion,

$$N(E, x) = \text{Re} \left[\frac{E}{\sqrt{E^2 - \Phi(E, x)\Phi^\dagger(E, x)}} \right], \quad (42)$$

where $\Phi^\dagger(E, x) = \Phi^*(-E, x)$. Expanding $\Phi_s(E, x)$ and taking into account that Δ_{s0} is selected real, we obtain the proximity-induced correction to the s -wave DoS

$$\delta N_s(E, x) \approx \text{Re} \left[\frac{E\Delta_{s0} (\tilde{\Phi}_s^\dagger(E, x) + \tilde{\Phi}_s(E, x))}{2(E^2 - \Delta_{s0}^2)^{3/2}} \right] \quad (43)$$

The correction to the Green's function can be represented again as a Fourier series, $\tilde{\Phi}_s(E, x) = \sum_{m=0}^{\infty} \tilde{\Phi}_{s,m}(E) \cos(m\pi x/d_s)$. In the Matsubara presentation, two contributions to the Fourier components $\tilde{\Phi}_{s,m}$ are given by Eqs. (A8) and (A9). Using these results, we

obtain for these contributions at real energies,

$$\begin{aligned} \frac{\tilde{\Phi}_{s,b,m} + \tilde{\Phi}_{s,b,m}^\dagger}{2} &= \frac{(2 - \delta_m)\xi_{s,\Delta}^2 (d_s \xi_s^*)}{\sqrt{E^2 - \Delta_{s0}^2/\Delta_{s0} + i(\pi m \xi_{s,\Delta}/d_s)^2}} \\ &\times \sum_{\alpha} \frac{\sqrt{E^2 - \Delta_{s0}^2}}{\sqrt{|\Delta_{\alpha 0}|^2 - E^2}} \frac{\text{Re}[\Delta_{\alpha 0}] - \Delta_{s0}}{\tilde{\gamma}_{B\alpha}}, \\ \frac{\tilde{\Phi}_{s,\Delta,m} + \tilde{\Phi}_{s,\Delta,m}^\dagger}{2} &= \frac{\sqrt{E^2 - \Delta_{s0}^2} \tilde{\Delta}_{s,m}^R}{\sqrt{E^2 - \Delta_{s0}^2 + i\Delta_{s0}(\pi m \xi_{s,\Delta}/d_s)^2}}, \end{aligned}$$

where $\tilde{\Delta}_{s,m}^R$ is given by Eq. (13a). These results together with Eq. (43) determine the shape of the DoS correction for arbitrary parameters of superconductors in the linear approximation with respect to the coupling strength $1/\tilde{\gamma}_{B\alpha}$.

For the important case of small d_s we can keep only the uniform $m=0$ term in the Fourier expansions leading to a simple result similar to one for the aligned state²²,

$$\frac{\tilde{\Phi}_{s,b,m} + \tilde{\Phi}_{s,b,m}^\dagger}{2} = \sum_{\alpha} \Gamma_{B,\alpha} \frac{\text{Re}[\Delta_{\alpha 0}] - \Delta_{s0}}{\sqrt{|\Delta_{\alpha 0}|^2 - E^2}} \quad (44)$$

with

$$\Gamma_{B,\alpha} = \Delta_{s0} \frac{\xi_{s,\Delta}^2}{d_s \xi_s^* \tilde{\gamma}_{B\alpha}} = \frac{1}{2e^2 \nu_s d_s R_B^\alpha}.$$

Therefore, the correction to the s -wave DoS in the case of thin s -wave layer is given by,

$$\begin{aligned} \delta N_s(E, x) &\approx \frac{E\Delta_{s0}}{(E^2 - \Delta_{s0}^2)^{3/2}} \sum_{\alpha} \Gamma_{B\alpha} \\ &\times \frac{\text{Re}[\Delta_{\alpha 0}] - \Delta_{s0}}{\sqrt{|\Delta_{\alpha 0}|^2 - E^2}} \Theta(|\Delta_{\alpha 0}| - E), \quad (45) \end{aligned}$$

where $\Theta(x)$ is the step function. If, as before, we define that phase shift between Δ_{s0} and Δ_{10} as ϕ then $\text{Re}[\Delta_{10}] = |\Delta_{10}| \cos \phi$ and $\text{Re}[\Delta_{20}] = -|\Delta_{20}| \cos \phi$.

Figure 4 illustrates the evolution of this correction with increasing angle ϕ for representative parameters. Two limiting cases $\phi = 0$ and π correspond to aligned states in which the aligned and anti-aligned gaps induce asymmetric peak and dip correspondingly. With increasing phase, the peak smoothly transforms into a dip and vice versa. In the maximally frustrated state for $\phi = \pi/2$ the DoS has two small dips. Note that the DoS correction is obtained with the linear approximation with respect to the coupling between the superconductors, which somewhat overestimates the amplitude and sharpness of the peaks.²²

VIII. SUMMARY AND DISCUSSION

In summary, we evaluated the range of parameters where the TRSB state is realized for the interface between s -wave and s_{\pm} superconductors using the simple

microscopic theory. This state appears when the partial Josephson energies almost completely compensate each other. The width of the TRSB region is determined by the $\sin(2\phi)$ term in the Josephson current, which appears in the second order with respect to the coupling strength between the superconductors. We found that the dominating contribution to this term is determined by the direct boundary correction to the Green's function of the s_{\pm} superconductor. This term is missed by phenomenological models of the junction. The width of the TRSB region shrinks with increasing temperature giving possibility to detect the transition from the aligned to TRSB state as function of temperature.

The main purpose of this paper is to establish factors which determine the width of the TRSB region at the s/s_{\pm} interface in the simplest possible situation accessible for full analytical analysis. Even in this relatively simple case the analysis occurred to be very nontrivial.

Several factors may have quantitative influence on results reported in this paper and complicate their applications to real iron-based superconductors:

- Most of these materials have more than two bands (up to five). This is not a crucial complication. Our consideration can be directly generalized to arbitrary number of bands.
- Due to the very short coherence length, most iron-based superconductors are probably in the clean limit. In the cleanest materials a significant anisotropy of the gap³⁶ and even the gap nodes³⁷ were revealed. On the other hand, in several other compounds isotropic gaps within the bands were found³⁸, which probably indicates substantial intraband scattering. The presence of a significant gap anisotropy and nodes does not contradict an overall picture of the s_{\pm} state because what matters most is the average gap inside the band. This means that the TRSB state is also expected within some range of parameters at the interface between conventional and clean s_{\pm} superconductor. However, our calculation of the width of this region is not directly applicable to this case.
- In compounds with strong impurity scattering one can expect some interband scattering, which was neglected in our model. As this scattering suppresses s_{\pm} state, it can not be too strong. The main effects of this scattering are suppression of the s_{\pm} gap parameters and emergence of the sub-gap states. These effect may have some influence on the location and width of the TRSB region.

An accurate description of these factors requires special considerations that will further complicate the theoretical model. Nevertheless, we expect that a qualitative picture of the transitional region will hold within a more realistic framework.

ACKNOWLEDGMENTS

I acknowledge many useful discussions with Valentin Stanev and Thomas Proslir. This work was supported by UChicago Argonne, LLC, operator of Argonne National Laboratory, a U.S. Department of Energy Office of Science laboratory, operated under contract No. DE-AC02-06CH11357, and by the "Center for Emergent Superconductivity", an Energy Frontier Research Center funded by the U.S. Department of Energy, Office of Science, Office of Basic Energy Sciences under Award Number DE-AC0298CH1088.

Appendix A: Derivation of boundary-induced corrections in the weak-coupling limit

In this Appendix we derive corrections to the Green's functions and gaps in the linear order with respect to the coupling parameters $1/\gamma_{B\alpha}$. As a zero approximation, we consider a general complex case when there is a finite phase difference ϕ between the bulk zero-order gap parameters Δ_{10} and Δ_{s0} as shown in Fig. 2. Correspondingly, the phase difference between Δ_{20} and Δ_{s0} is $\phi - \pi$. This calculation covers both aligned states when ϕ equals 0 or π and complex TRSB states with $0 < \phi < \pi$.

1. s -wave gap and Green's function

We start with calculation of corrections to the s -wave Green's functions and gap parameter, $\tilde{\Phi}_s$ and $\tilde{\Delta}_s$. From Eq. (4a) we obtain that the first-order corrections to the s -wave Green's functions obeys the following equations

$$\xi_{s,\omega}^2 \frac{d^2 \tilde{\Phi}_s}{dx^2} - \tilde{\Phi}_s = -\tilde{\Delta}_s, \quad (\text{A1})$$

where $\xi_{s,\omega}^2 = D_s / (2\sqrt{\omega^2 + \Delta_{s0}^2}) = \xi_{s,\Delta}^2 \Delta_{s0} / \sqrt{\omega^2 + \Delta_{s0}^2}$ and $\xi_{s,\Delta}^2 = D_s / (2\Delta_{s0})$. Without loss of generality, the zero-order gap parameters Δ_{s0} can be selected real. In this case the self-consistency condition for the linear corrections can be written as

$$2\pi T \sum_{\omega>0} \frac{1}{\sqrt{\omega^2 + \Delta_{s0}^2}} \left(\tilde{\Phi}_s - \frac{\Delta_{s0}^2 \text{Re}[\tilde{\Phi}_s]}{\omega^2 + \Delta_{s0}^2} - \tilde{\Delta}_s \right) = 0. \quad (\text{A2})$$

In the boundary condition for $d\Phi_s/dx$, Eq. (6a), we can neglect in the right hand side differences between Φ 's and Δ 's and approximate Δ 's by their bulk values. This gives

$$\frac{\xi_s^*}{\sqrt{\omega^2 + \Delta_{s0}^2}} \frac{d\tilde{\Phi}_s}{dx} = - \sum_{\alpha} \frac{1}{\tilde{\gamma}_{B\alpha}} \frac{\Delta_{s0} - \Delta_{\alpha 0}}{\sqrt{\omega^2 + |\Delta_{\alpha 0}|^2}} \quad (\text{A3})$$

at $x = 0$. Note that, in general, $\tilde{\Delta}_s$, $\tilde{\Phi}_s$, and $\Delta_{\alpha 0}$ are complex, $\Delta_{\alpha 0} = |\Delta_{\alpha 0}| \exp(i\phi_{\alpha})$, $\phi_1 = \phi$, $\phi_2 = \phi - \pi$. They are real only for the aligned state.

To solve Eqs. (A1) and (A3) it is convenient to split $\tilde{\Phi}_s$ into the two contributions, $\tilde{\Phi}_s = \tilde{\Phi}_{s,b} + \tilde{\Phi}_{s,\Delta}$, where $\tilde{\Phi}_{s,b}$ is induced by the boundary condition and $\tilde{\Phi}_{s,\Delta}$ is induced by the gap correction. The first contribution $\tilde{\Phi}_{s,b}$ can be found from the following equation and the boundary condition

$$\xi_{s,\omega}^2 \tilde{\Phi}_{s,b}'' - \tilde{\Phi}_{s,b} = 0, \quad (\text{A4a})$$

$$\xi_s^* \tilde{\Phi}'_{s,b}(0) = \sum_{\alpha} \frac{1}{\tilde{\gamma}_{B\alpha}} \frac{\sqrt{\omega^2 + \Delta_{s0}^2}}{\sqrt{\omega^2 + |\Delta_{\alpha 0}|^2}} (\Delta_{\alpha 0} - \Delta_{s0}), \quad (\text{A4b})$$

while the second contribution, $\tilde{\Phi}_{s,\Delta}$, obeys

$$\xi_{s,\omega}^2 \tilde{\Phi}_{s,\Delta}'' - \tilde{\Phi}_{s,\Delta} = -\tilde{\Delta}_s, \quad (\text{A5a})$$

$$\tilde{\Phi}'_{s,\Delta}(0) = 0. \quad (\text{A5b})$$

The solution $\tilde{\Phi}_{s,b}(x)$ of the linear equation (A4a) with the boundary condition $\tilde{\Phi}'_{s,b} = 0$ at $x = -d_s$ is given by

$$\tilde{\Phi}_{s,b}(x) = C_{s,b} \cosh\left(\frac{x + d_s}{\xi_{s,\omega}}\right), \quad (\text{A6})$$

where the constant $C_{s,b}$ can be found from the boundary condition at $x = 0$, Eq. (A4b),

$$C_{s,b} = \frac{\xi_{s,\omega}/\xi_s^*}{\sinh(d_s/\xi_{s,\omega})} \sum_{\alpha} \frac{\sqrt{\omega^2 + \Delta_{s0}^2}}{\tilde{\gamma}_{B\alpha} \sqrt{\omega^2 + |\Delta_{\alpha 0}|^2}} (\Delta_{\alpha 0} - \Delta_{s0})$$

leading to the following result

$$\begin{aligned} \tilde{\Phi}_{s,b}(x) &= \frac{\xi_{s,\omega} \cosh[(x + d_s)/\xi_{s,\omega}]}{\xi_s^* \sinh(d_s/\xi_{s,\omega})} \\ &\times \sum_{\alpha} \frac{\sqrt{\omega^2 + \Delta_{s0}^2}}{\tilde{\gamma}_{B\alpha} \sqrt{\omega^2 + |\Delta_{\alpha 0}|^2}} (\Delta_{\alpha 0} - \Delta_{s0}). \end{aligned} \quad (\text{A7})$$

We compute $\tilde{\Phi}_{s,\Delta}$ and $\tilde{\Delta}_s$ using the Fourier expansions, $\tilde{\Phi}_{s,\Delta}(x) = \sum_{m=0}^{\infty} \tilde{\Phi}_{s,\Delta,m} \cos k_m x$, $\tilde{\Delta}_s(x) = \sum_{m=0}^{\infty} \tilde{\Delta}_{s,m} \cos k_m x$ with $k_m = m\pi/d_s$. The Fourier components $\tilde{\Phi}_{s,b,m}$ of $\tilde{\Phi}_{s,b}(x)$ can be computed explicitly from Eq. (A7),

$$\tilde{\Phi}_{s,b,m} = \frac{(2 - \delta_m) \xi_{s,\omega}^2 / (d_s \xi_s^*)}{1 + \xi_{s,\omega}^2 k_m^2} \sum_{\alpha} \frac{\sqrt{\omega^2 + \Delta_{s0}^2}}{\sqrt{\omega^2 + |\Delta_{\alpha 0}|^2}} \frac{\Delta_{\alpha 0} - \Delta_{s0}}{\tilde{\gamma}_{B\alpha}}. \quad (\text{A8})$$

Eq. (A5a) immediately gives the following relation between the Fourier components $\tilde{\Phi}_{s,\Delta,m}$ and $\tilde{\Delta}_{s,m}$

$$\tilde{\Phi}_{s,\Delta,m} = \frac{\tilde{\Delta}_{s,m}}{1 + \xi_{s,\omega}^2 k_m^2}. \quad (\text{A9})$$

Substituting this result into the self-consistency condition (A2) and splitting it into the real and imaginary parts, we relate $\tilde{\Delta}_{s,m} = \tilde{\Delta}_{s,m}^R + i\tilde{\Delta}_{s,m}^I$ to $\tilde{\Phi}_{s,b,m} =$

$\tilde{\Phi}_{s,b,m}^R + i\tilde{\Phi}_{s,b,m}^I$ as

$$2\pi T \sum_{\omega>0} \frac{\Delta_{s0}^2 + \omega^2}{(\omega^2 + \Delta_{s0}^2)^{3/2}} \frac{\xi_{s,\omega}^2 k_m^2}{1 + \xi_{s,\omega}^2 k_m^2} \tilde{\Delta}_{s,m}^R = 2\pi T \sum_{\omega>0} \frac{\omega^2 \tilde{\Phi}_{s,b,m}^R}{(\omega^2 + \Delta_{s0}^2)^{3/2}}, \quad (\text{A10a})$$

$$2\pi T \sum_{\omega>0} \frac{1}{\sqrt{\omega^2 + \Delta_{s0}^2}} \frac{\xi_{s,\omega}^2 k_m^2}{1 + \xi_{s,\omega}^2 k_m^2} \tilde{\Delta}_{s,m}^I = 2\pi T \sum_{\omega>0} \frac{\tilde{\Phi}_{s,b,m}^I}{\sqrt{\omega^2 + \Delta_{s0}^2}}. \quad (\text{A10b})$$

The components $\tilde{\Delta}_{s,m}^R$ and $\tilde{\Delta}_{s,m}^I$ describe responses of the s-wave gap parameter to the interface perturbation in the amplitude and phase channels. Eqs. (A8), (A9), and (A10) already provide a formal solution of the problem. As the left hand side of Eq. (A10b) vanishes for $m = 0$, solution for the imaginary part exists only if

$$\sum_{\omega>0} \frac{\tilde{\Phi}_{s,b,0}^I}{\sqrt{\omega^2 + \Delta_{s0}^2}} = 0$$

giving the condition

$$\sum_{\alpha, \omega>0} \frac{1}{\sqrt{\omega^2 + \Delta_{s0}^2} \sqrt{\omega^2 + |\Delta_{\alpha 0}|^2}} \frac{\text{Im}[\Delta_{\alpha 0}]}{\tilde{\gamma}_{B\alpha}} = 0. \quad (\text{A11})$$

Uncertainty in $\tilde{\Delta}_{s,0}^I$ reflects the phase-rotation invariance and we can select $\tilde{\Delta}_{s,0}^I = 0$. As the Josephson energy between the s-wave superconductor and α band, $E_{J\alpha}$ is given by Eq. (11) and $\Delta_{\alpha 0} = |\Delta_{\alpha 0}| \exp(i\phi_{\alpha})$, we can see that the condition (A11) simply means

$$\sum_{\alpha} E_{J\alpha} \sin \phi_{\alpha} = 0.$$

Since the partial Josephson currents are proportional to $E_{J\alpha}$, this condition implies that the total Josephson current flowing through the boundary is always zero in the ground state. For two bands the condition for realization of the TRSB state *in the linear order with respect to the interface transparency* is simply $E_{J1} = E_{J2}$. To establish an accurate range of parameters within which the TRSB state is stable, one has to go beyond the linear order.

Using the expansion (A8), we obtain the explicit representations for $\tilde{\Delta}_{s,m}^R$ and $\tilde{\Delta}_{s,m}^I$ given by Eqs. (13) of the main text which in turn determine the term $\tilde{\Phi}_{s,\Delta,m}$ of the Green's function, Eq. (A9). Since we already derived the result for $\tilde{\Phi}_{s,b,m}$, Eq. (A7), we now have all corrections.

The full analytical formulas are somewhat cumbersome and it is useful to derive more transparent results in simple limiting cases. At low temperatures the summation with respect to the Matsubara frequencies can be replaced by the integration $2\pi T \sum_{\omega>0} \rightarrow \int_0^{\infty} d\omega$. In this limit we can obtain the analytical result for the average correction to the order parameter amplitude, $\tilde{\Delta}_{s,0}^R$,

$$\frac{\tilde{\Delta}_{s,0}^R}{\pi T_c} = \frac{\xi_s^*}{d_s} \sum_{\alpha} U(\Delta_{s0}/|\Delta_{\alpha 0}|) \frac{\text{Re}[\Delta_{\alpha 0}] - \Delta_{s0}}{\tilde{\gamma}_{B\alpha} |\Delta_{\alpha 0}|} \quad (\text{A12})$$

with

$$U(a) = \int_0^\infty dz \frac{z^2}{(z^2+1)^{3/2} \sqrt{a^2 z^2 + 1}} = \frac{K(1-a^2) - E(1-a^2)}{1-a^2},$$

where $K(m) = \int_0^{\pi/2} (1-m \sin^2 \theta)^{-1/2} d\theta$ and $E(m) = \int_0^{\pi/2} (1-m \sin^2 \theta)^{1/2} d\theta$ are the complete elliptic integrals. As we mentioned before, the uniform part of $\tilde{\Delta}_s$ can be selected to be real, $\tilde{\Delta}_{s,0} = \tilde{\Delta}_{s,0}^R$.

We can derive the simple analytical results for important particular case of (i) thin s -layer, $d_s \ll \xi_{s,\Delta}$, (ii) weaker s -superconductor, $\Delta_{s0} \ll |\Delta_{\alpha 0}|$, and (iii) low temperatures, $T \ll T_c^s$. Due to the first condition, the dominating contribution to the gap correction is given by the coordinate independent part $\tilde{\Delta}_{s,0}$, which is determined by the general formula (A12). In the limit of $\Delta_{s0} \ll |\Delta_{\alpha 0}|$ we can use the asymptotics of the function $U(a)$ in the limit $a \ll 1$, $U(a) \approx \ln(4/a) - 1$, leading to the following simple result

$$\frac{\tilde{\Delta}_{s,0}^R}{\pi T_c} \approx \frac{\xi_s^*}{d_s} \sum_\alpha \frac{\text{Re}[\Delta_{\alpha 0}] - \Delta_{s0}}{\tilde{\gamma}_{B\alpha} |\Delta_{\alpha 0}|} \left[\ln \left(\frac{4|\Delta_{\alpha 0}|}{\Delta_{s0}} \right) - 1 \right]. \quad (\text{A13})$$

The sign of $\tilde{\Delta}_{s,0}^R$ determines net effect of the s_\pm superconductor on the s superconductor, i.e., the sign of the proximity effect (positive vs negative proximity). The proximity is always negative in the TRSB state. In the case of the aligned state corresponding to $\text{Re}[\Delta_{\alpha 0}] = \Delta_{\alpha 0}$, as one can expect, s_\pm gaps aligned with Δ_{s0} enhance s -wave superconductivity while anti-aligned s_\pm gaps suppress superconductivity in the s superconductor. The relative contributions are mostly determined by the electrical coupling between s -superconductor and the s_\pm bands described by parameters $\tilde{\gamma}_{B\alpha}^{-1}$. Another important factor is that the aligned gaps give positive contribution proportional to gap difference $\Delta_{\alpha 0} - \Delta_{s0}$, while antialigned gaps give negative contribution proportional to gap sum $|\Delta_{\alpha 0}| + \Delta_{s0}$. This give possibility to total negative proximity effect in the aligned state.

Weak spatial dependence of $\tilde{\Delta}_s(x)$ is determined by the components $\tilde{\Delta}_{s,m}$ with $m > 0$. At $T = 0$ these components can be presented as

$$\tilde{\Delta}_{s,m}^R = \frac{1}{Z_{s,m}^a} \frac{2\xi_{s,\Delta}^2}{d_s \xi_s^*} \sum_\alpha J_a \left(\frac{|\Delta_{\alpha 0}|}{\Delta_{s0}}, \beta_m \right) \frac{\text{Re}[\Delta_{\alpha 0}] - \Delta_{s0}}{\tilde{\gamma}_{B\alpha}}, \quad (\text{A14a})$$

$$\tilde{\Delta}_{s,m}^I = \frac{1}{Z_{s,m}^\phi} \frac{2\xi_{s,\Delta}^2}{d_s \xi_s^*} \sum_\alpha J_\phi \left(\frac{|\Delta_{\alpha 0}|}{\Delta_{s0}}, \beta_m \right) \frac{\text{Im}[\Delta_{\alpha 0}]}{\tilde{\gamma}_{B\alpha}} \quad (\text{A14b})$$

with $\beta_m = (\pi m \xi_{s,\Delta} / d_s)^2$,

$$\begin{aligned} Z_{s,m}^a &= \int_0^\infty \frac{dz}{(z^2+1)^{3/2}} \left[1 + \frac{\beta_m z^2}{\sqrt{z^2+1} + \beta_m} \right] \\ &= \frac{1}{\beta_m} \left[\frac{\pi}{2} + \sqrt{\beta_m^2 - 1} \ln \left(\sqrt{\beta_m^2 - 1} + \beta_m \right) \right], \\ J_a(\delta, \beta) &= \int_0^\infty dz \frac{z^2}{(z^2+1) \sqrt{z^2+\delta^2}} \frac{1}{\sqrt{z^2+1} + \beta}, \\ Z_{s,m}^\phi &= \int_0^\infty \frac{dz}{\sqrt{z^2+1}} \frac{\beta_m}{\sqrt{z^2+1} + \beta_m} \\ &= \frac{\beta_m}{\sqrt{\beta_m^2 - 1}} \ln \left(\beta_m + \sqrt{\beta_m^2 - 1} \right), \\ J_\phi(\delta, \beta) &= \int_0^\infty \frac{dz}{\sqrt{z^2+\delta^2} (\sqrt{z^2+1} + \beta)}. \end{aligned}$$

In the limit $\beta_m \gg 1$ corresponding to $d_s \ll \xi_s$, asymptotics of both $Z_{s,m}^a$ and $Z_{s,m}^\phi$ are $Z_{s,m}^{\{a,\phi\}} \approx \ln(2\beta_m)$. In the limits $|\Delta_{\alpha 0}| \gg \Delta_{s0}$ and $\Delta_{s0} \beta_m \gg |\Delta_{\alpha 0}|$ corresponding to $\beta \gg \delta \gg 1$, $J_a(\delta, \beta)$ and $J_\phi(\delta, \beta)$ also have the same asymptotics

$$J_{\{a,\phi\}}(\delta, \beta) \approx \int_0^\infty \frac{dz}{(z+\beta) \sqrt{z^2+\delta^2}} \approx \frac{1}{\beta} \ln \frac{2\beta}{\delta}.$$

Collecting all terms, we obtain

$$\tilde{\Delta}_{s,m} \approx \sum_\alpha \left[1 + \frac{\ln(\Delta_{s0}/|\Delta_{\alpha 0}|)}{\ln \left[2(\pi m \xi_{s,\Delta}/d_s)^2 \right]} \right] \frac{2d_s/\xi_s^*}{(\pi m)^2} \frac{\Delta_{\alpha 0} - \Delta_{s0}}{\tilde{\gamma}_{B\alpha}}.$$

Using the relation $(|x|-1)^2 = \frac{1}{3} + 4 \sum_{m=1}^\infty \frac{\cos(\pi m x)}{(\pi m)^2}$, we can approximately present the gap correction in real space as

$$\begin{aligned} \tilde{\Delta}_s(x) &\approx \tilde{\Delta}_{s,0} - \frac{d_s}{\xi_s^*} \sum_\alpha \frac{\Delta_{\alpha 0} - \Delta_{s0}}{\tilde{\gamma}_{B\alpha}} \left[\frac{(x+d_s)^2}{2d_s^2} - \frac{1}{6} \right] \\ &\times \left[1 + \frac{\ln(\Delta_{s0}/|\Delta_{\alpha 0}|)}{2 \ln(\pi \sqrt{2} \xi_{s,\Delta}/d_s)} \right]. \quad (\text{A15}) \end{aligned}$$

Correspondingly, for the Green's function in the same limits we derive

$$\begin{aligned} \tilde{\Phi}_s(\omega, x) &\approx \tilde{\Delta}_{s,0} + \pi T_c \frac{\xi_s^*}{d_s} \left[1 + \frac{1}{2} \left(\frac{x+d_s}{\xi_{s,\omega}} \right)^2 \right] \\ &\times \sum_\alpha \frac{1}{\sqrt{\omega^2 + \Delta_\alpha^2}} \frac{\Delta_{\alpha 0} - \Delta_{s0}}{\tilde{\gamma}_{B\alpha}}. \quad (\text{A16}) \end{aligned}$$

In summary, simple analytical results given by Eqs. (A13), (A15), and (A16) determine corrections to the s -wave gap and Green's function for a thin s -wave layer.

2. s_\pm -wave gaps and Green's functions

We can evaluate corrections to the s_\pm gap parameters and Green's functions following the same general route.

The difference is that the matrix structure of the self-consistency condition, Eq. (5b), has to be properly accounted for. The first-order correction to $\tilde{\Phi}_\alpha$ with respect to the coupling strength $\gamma_{B\alpha}^{-1}$ is determined by the following equation and boundary conditions,

$$\xi_{\alpha,\omega}^2 \tilde{\Phi}_\alpha'' - \tilde{\Phi}_\alpha = -\tilde{\Delta}_\alpha, \quad (\text{A17a})$$

$$\xi_\alpha G_\alpha \tilde{\Phi}'_\alpha = \frac{G_s}{\gamma_{B\alpha}} (\Delta_{s0} - \Delta_{\alpha0}), \text{ at } x=0 \quad (\text{A17b})$$

and $\tilde{\Phi}'_\alpha = 0$ at $x=d_\pm$ with $G_\alpha \approx \omega/\sqrt{\omega^2+|\Delta_{\alpha0}|^2}$, $\xi_{\alpha,\omega}^2 = D_\alpha/(2\sqrt{\omega^2+|\Delta_{\alpha0}|^2}) = \xi_{\alpha,\Delta}^2 |\Delta_{\alpha0}|/\sqrt{\omega^2+|\Delta_{\alpha0}|^2}$, and $\xi_{\alpha,\Delta}^2 \equiv D_\alpha/(2|\Delta_{\alpha0}|)$. The self-consistency condition for corrections can be written as

$$2\pi T \sum_{\omega>0} \left[\frac{1}{\sqrt{\omega^2+|\Delta_{\alpha0}|^2}} \left(\tilde{\Phi}_\alpha - \frac{\Delta_{\alpha0} \text{Re} [\tilde{\Phi}_\alpha \Delta_{\alpha0}^*]}{\omega^2+|\Delta_{\alpha0}|^2} \right) - \frac{\tilde{\Delta}_\alpha}{\omega} \right] \\ = \sum_\beta w_{\alpha\beta} \tilde{\Delta}_\beta - \ln \frac{T_c}{T} \tilde{\Delta}_\alpha \quad (\text{A18})$$

with $w_{\alpha\beta} = \lambda_{\alpha\beta}^{-1} - \lambda^{-1} \delta_{\alpha\beta}$ and λ is the largest eigenvalue of the matrix $\lambda_{\alpha\beta}$. The matrix $w_{\alpha\beta}$ is degenerate, $w_{11}w_{22} - w_{12}w_{21} = 0$, and its components are given by

$$\begin{pmatrix} w_{11} \\ w_{22} \end{pmatrix} = \frac{\sqrt{\lambda_-^2/4 + \lambda_{12}\lambda_{21}} \mp \lambda_-/2}{\det \lambda}, \quad w_{12} = -\frac{\lambda_{12}}{\det \lambda} \quad (\text{A19})$$

with $\lambda_- \equiv \lambda_{11} - \lambda_{22}$ and $\det \lambda \equiv \lambda_{11}\lambda_{22} - \lambda_{12}\lambda_{21}$.

Similar to the s -wave case, we can split $\tilde{\Phi}_\alpha$ into the contributions induced by the boundary condition and by the correction to the gap parameter, $\tilde{\Phi}_\alpha = \tilde{\Phi}_{\alpha,b} + \tilde{\Phi}_{\alpha,\Delta}$. The equation and the boundary condition for $\tilde{\Phi}_{\alpha,b}(x)$ are

$$\xi_{\alpha,\omega}^2 \tilde{\Phi}_{\alpha,b}'' - \tilde{\Phi}_{\alpha,b} = 0, \quad (\text{A20a})$$

$$\xi_\alpha \tilde{\Phi}'_{\alpha,b} = -\frac{1}{\gamma_{B\alpha}} \frac{\sqrt{\omega^2+|\Delta_{\alpha0}|^2}}{\sqrt{\omega^2+\Delta_{s0}^2}} (\Delta_{s0} - \Delta_{\alpha0}). \quad (\text{A20b})$$

The solution for $\tilde{\Phi}_{\alpha,b}(x)$ is given by

$$\tilde{\Phi}_{\alpha,b}(x) = \frac{\xi_{\alpha,\omega}}{\xi_\alpha} \frac{\sqrt{\omega^2+|\Delta_{\alpha0}|^2}}{\gamma_{B\alpha} \sqrt{\omega^2+\Delta_{s0}^2}} \\ \times \frac{\cosh [(x-d_\pm)/\xi_{\alpha,\omega}]}{\sinh (d_\pm/\xi_{\alpha,\omega})} (\Delta_{s0} - \Delta_{\alpha0}). \quad (\text{A21})$$

The component $\tilde{\Phi}_{\alpha,\Delta}(x)$ has to be found from the following equation and boundary conditions

$$\xi_{\alpha,\omega}^2 \tilde{\Phi}_{\alpha,\Delta}'' - \tilde{\Phi}_{\alpha,\Delta} = -\tilde{\Delta}_\alpha, \quad (\text{A22a})$$

$$\tilde{\Phi}'_{\alpha,\Delta} = 0 \text{ for } x=0, d_\pm. \quad (\text{A22b})$$

We can again find $\tilde{\Phi}_{\alpha,\Delta}(x)$ and $\tilde{\Delta}_\alpha(x)$ using Fourier expansions, $\tilde{\Phi}_{\alpha,\Delta}(x) = \sum_m \tilde{\Phi}_{\alpha,\Delta,m} \cos(q_m x)$, $\tilde{\Delta}_\alpha(x) =$

$\sum_m \tilde{\Delta}_{\alpha,m} \cos(q_m x)$ with $q_m = m\pi/d_\pm$. From Eq. (A22a) we immediately find

$$\tilde{\Phi}_{\alpha,\Delta,m} = \frac{\tilde{\Delta}_{\alpha,m}}{1 + \xi_{\alpha,\omega}^2 q_m^2}. \quad (\text{A23})$$

As follows from the structure of the the self-consistency equation (A18), the responses of the order parameters $\tilde{\Delta}_\alpha$ are different in the amplitude and phase channels. To proceed, we split all quantities into the amplitude and phase components, as illustrated in Fig. 2, $X = X^a + X^\phi$,

$$X^a = \frac{\Delta_{\alpha0} \text{Re}[X \Delta_{\alpha0}^*]}{|\Delta_{\alpha0}|^2}; \quad X^\phi = X - \frac{\Delta_{\alpha0} \text{Re}[X \Delta_{\alpha0}^*]}{|\Delta_{\alpha0}|^2},$$

where X stands for $\tilde{\Delta}_\alpha$, $\tilde{\Phi}_{\alpha,b}$, $\tilde{\Phi}_{\alpha,\Delta}$, and Δ_{s0} . Such decomposition of Δ_{s0} is illustrated in Fig. 2. Explicitly, we can write, $\Delta_{s0}^a = (\Delta_{10}/|\Delta_{10}|)|\Delta_{s0}| \cos \phi$ and $\Delta_{s0}^\phi = -i(\Delta_{10}/|\Delta_{10}|)|\Delta_{s0}| \sin \phi$. Substituting $\tilde{\Phi}_{\alpha,\Delta}$ into the self-consistency equation (A18), we obtain the following equations for $\tilde{\Delta}_{\alpha,m}^a$ and $\tilde{\Delta}_{\alpha,m}^\phi$

$$\sum_\beta (w_{\alpha\beta} - \Sigma_{\alpha,m}^a \delta_{\alpha\beta}) \tilde{\Delta}_{\beta,m}^a = 2\pi T \sum_{\omega>0} \frac{\omega^2 \tilde{\Phi}_{\alpha,b,m}^a}{(\omega^2+|\Delta_{\alpha0}|^2)^{3/2}}, \quad (\text{A24a})$$

$$\Sigma_{\alpha,m}^a = 2\pi T \sum_{\omega>0} \left[\frac{\omega^2}{(\omega^2+|\Delta_{\alpha0}|^2)^{3/2} (1+\xi_{\alpha,\omega}^2 q_m^2)} - \frac{1}{\omega} \right] + \ln \frac{T_c}{T},$$

$$\sum_\beta (w_{\alpha\beta} - \Sigma_{\alpha,m}^\phi \delta_{\alpha\beta}) \tilde{\Delta}_{\beta,m}^\phi = 2\pi T \sum_{\omega>0} \frac{\tilde{\Phi}_{\alpha,b,m}^\phi}{\sqrt{\omega^2+|\Delta_{\alpha0}|^2}}, \quad (\text{A24b})$$

$$\Sigma_{\alpha,m}^\phi = 2\pi T \sum_{\omega>0} \left[\frac{1}{\sqrt{\omega^2+|\Delta_{\alpha0}|^2}} \frac{1}{1+\xi_{\alpha,\omega}^2 q_m^2} - \frac{1}{\omega} \right] + \ln \frac{T_c}{T},$$

where the Fourier components $\tilde{\Phi}_{\alpha,b,m}^a$ and $\tilde{\Phi}_{\alpha,b,m}^\phi$ can be computed explicitly from Eq. (A21),

$$\begin{pmatrix} \tilde{\Phi}_{\alpha,b,m}^a \\ \tilde{\Phi}_{\alpha,b,m}^\phi \end{pmatrix} = \frac{(2-\delta_m) \xi_{\alpha,\omega}^2 / (d_\pm \xi_\alpha)}{\gamma_{B\alpha} (1+\xi_{\alpha,\omega}^2 q_m^2)} \\ \times \frac{\sqrt{\omega^2+|\Delta_{\alpha0}|^2}}{\sqrt{\omega^2+\Delta_{s0}^2}} \begin{pmatrix} \Delta_{s0}^a - \Delta_{\alpha0} \\ \Delta_{s0}^\phi \end{pmatrix}. \quad (\text{A25})$$

Solutions of Eqs. (A24) are

$$\tilde{\Delta}_{\alpha,m}^a = 2\pi T \sum_{\beta,\omega>0} U_{m,\alpha\beta}^a \frac{\omega^2 \tilde{\Phi}_{\beta,b,m}^a}{(\omega^2+|\Delta_{\beta0}|^2)^{3/2}}, \quad (\text{A26a})$$

$$\tilde{\Delta}_{\alpha,m}^\phi = 2\pi T \sum_{\beta,\omega>0} U_{m,\alpha\beta}^\phi \frac{\tilde{\Phi}_{\beta,b,m}^\phi}{\sqrt{\omega^2+|\Delta_{\beta0}|^2}}, \quad (\text{A26b})$$

where the matrices $U_{m,\alpha\beta}^{a,\phi} = [w_{\alpha\beta} - \Sigma_{\alpha,m}^{a,\phi} \delta_{\alpha\beta}]^{-1}$ in the two-band case are given by

$$U_{m,\alpha\beta}^{a,\phi} = \frac{1}{D_{U,m}^{a,\phi}} \begin{bmatrix} w_{22} - \Sigma_{2,m}^{a,\phi} & -w_{12} \\ -w_{21} & w_{11} - \Sigma_{1,m}^{a,\phi} \end{bmatrix}, \quad (\text{A27})$$

$$D_{U,m}^{a,\phi} = -\Sigma_{2,m}^{a,\phi} w_{11} - \Sigma_{1,m}^{a,\phi} w_{22} + \Sigma_{1,m}^{a,\phi} \Sigma_{2,m}^{a,\phi}.$$

The equation for the phase component at $m = 0$ requires special attention. We note that the equation for the bulk gaps have the form

$$\sum_{\beta} \left(w_{\alpha\beta} - \Sigma_{\alpha,0}^{\phi} \delta_{\alpha\beta} \right) \Delta_{\beta 0} = 0$$

meaning that Eq. (A24b) at $m = 0$ is actually degenerate, i.e., its determinant vanishes, $D_{U,0}^{a,\phi} = -w_{11}\Sigma_{2,0}^{\phi} - w_2\Sigma_{1,0}^{\phi} + \Sigma_{1,0}^{\phi}\Sigma_{2,0}^{\phi} = 0$. This degeneracy reflects gauge invariance with respect to identical phase change of the order parameters $\Delta_{\alpha 0}$. This means that the equation for $\tilde{\Delta}_{\alpha,0}^{\phi}$ only has solution if its right-hand side satisfies certain condition which, using the bulk gap ratio $\Delta_{10}/\Delta_{20} = -w_{12}/(w_{11} - \Sigma_{1,0}^{\phi}) = -(w_{22} - \Sigma_{2,0}^{\phi})/w_{21}$, can be written as

$$2\pi T \sum_{\omega > 0} \left(\frac{w_{21}\Delta_{10}\tilde{\Phi}_{1,b,0}^{\phi}}{\sqrt{\omega^2 + |\Delta_{10}|^2}} + \frac{w_{12}\Delta_{20}\tilde{\Phi}_{2,b,0}^{\phi}}{\sqrt{\omega^2 + |\Delta_{20}|^2}} \right) = 0. \quad (\text{A28})$$

The meaning of this condition is that the total ‘‘torque’’ from the interface forcing uniform phase rotation of the s_{\pm} gap parameters has to vanish. Using the relation $w_{21}/w_{12} = \lambda_{21}/\lambda_{12} = \nu_1/\nu_2$ and Eq. (A25) we can rewrite this condition as

$$2\pi T \sum_{\alpha,\omega > 0} \frac{\xi_{\alpha,\omega}^2}{\xi_{\alpha}} \frac{\nu_{\alpha}\Delta_{\alpha 0}}{\sqrt{\omega^2 + \Delta_{s0}^2}} \frac{\Delta_{s0}^{\phi}}{\gamma_{B\alpha}} = 0.$$

with $\Delta_{s0}^{\phi} = \Delta_{s0} \sin \phi$. Moreover, for the combination $\xi_{\alpha,\omega}^2 \nu_{\alpha} / \xi_{\alpha}$ we obtain

$$\frac{\xi_{\alpha,\omega}^2 \nu_{\alpha}}{\xi_{\alpha}} \propto \frac{D_{\alpha} \nu_{\alpha}}{\xi_{\alpha} \sqrt{\omega^2 + |\Delta_{\alpha 0}|^2}} \propto \frac{1}{\gamma_{\alpha} \sqrt{\omega^2 + |\Delta_{\alpha 0}|^2}},$$

which allows us to present the condition in the form

$$2\pi T \sum_{\alpha,\omega > 0} \frac{1}{\tilde{\gamma}_{B\alpha}} \frac{\Delta_{\alpha 0} \sin \phi}{\sqrt{\omega^2 + |\Delta_{\alpha 0}|^2} \sqrt{\omega^2 + \Delta_{s0}^2}} = 0.$$

We immediately recognize that this condition is equivalent to Eq. (A11) (vanishing of the total Josephson current flowing through the interface). With this condition,

Eq. (A25) for $\tilde{\Delta}_{\alpha,0}^{\phi}$ determines interface-induced phase shifts $\varphi_{\alpha} \ll 1$ of the averaged order parameters with respect to zero-order phases ϕ and $\phi - \pi$, see Fig. 2. These phase shifts are defined by relation $\tilde{\Delta}_{\alpha,0}^{\phi} = i\varphi_{\alpha}\Delta_{\alpha 0}$. The same phase shifts appear in the phenomenological frustrated Josephson junction model. As the average phase shift $(\varphi_1 + \varphi_2)/2$ can be absorbed into ϕ , we can set it zero and take $\varphi_{1,2} = \pm\varphi/2$. From Eq. (A11), taking into account the above condition, we derive

$$\varphi = -\frac{2\pi T}{d_{\pm} w_{12} |\Delta_{20}|} \sum_{\omega > 0} \frac{\xi_{1,\omega}^2 / \xi_1}{\sqrt{\omega^2 + \Delta_{s0}^2}} \frac{|\Delta_{s0}|}{\gamma_{B1}} \sin \phi \quad (\text{A29})$$

One can verify that this result does not change with the switching of indices $1 \leftrightarrow 2$ in the right hand side. Using the expression for the partial Josephson energy, Eq. (11), this result can be rewritten as

$$\varphi = -\frac{E_{J,1}}{d_{\pm} \nu_1 w_{12} |\Delta_{20}| |\Delta_{10}|} \sin \phi. \quad (\text{A30})$$

For weak interband coupling, $|\lambda_{12}|, |\lambda_{21}| \ll \lambda_{11}, \lambda_{22}$, the parameter $\mathcal{E}_{12} = \nu_1 w_{12} |\Delta_{20}| |\Delta_{10}|$ represents the interband energy and this result coincides with the result obtained within the frustrated Josephson junction model in the case $E_{J,1} \ll d_{\pm} \mathcal{E}_{12}$. In this situation $w_{12} > 0$ and $\varphi < 0$. However, in contrast to this model, in a general situation the phases φ_{α} do not fully determine the energy of the s_{\pm} superconductor. Moreover, it was argued that for the iron-based superconductors the pairing is dominated by the interband coupling, i.e., the opposite inequality holds, $|\lambda_{12}|, |\lambda_{21}| \gg \lambda_{11}, \lambda_{22}$. In this case, as $\lambda_{12} < 0$ and $\lambda_{11}\lambda_{22} - \lambda_{12}\lambda_{21} < 0$, we have $w_{12} < 0$ meaning that $\varphi > 0$. Fig. 2 actually illustrates this situation. Using the results presented in this Appendix, we derive in the main text the amplitude of the $\sin 2\phi$ term in the Josephson current which determines the width of the TRSB state.

¹ D. C. Johnston, Adv. Phys. **59**, 803 (2010); J-P. Paglione and R. L. Green, Nature Phys. **6**, 645 (2010); P. C. Canfield and S. L. Bud’ko, Annu. Rev. Cond. Mat. Phys. **1**, 27 (2010).
² P. J. Hirschfeld, M. M. Korshunov, and I. I. Mazin, Rep. Prog. Phys., **74**, 124508 (2011); A. V. Chubukov, Annu. Rev. Cond. Mat. Phys. **3**, 57 (2012).
³ L. Boeri, O. V. Dolgov, and A. A. Golubov, Phys. Rev. Lett. **101**, 026403 (2008); A. Subedi, L. Zhang, D. J. Singh, and M. H. Du, Phys. Rev. B **78**, 134514 (2008); T. Yildirim, Phys. Rev. Lett. **102**, 037003 (2009).

⁴ I. I. Mazin, D. J. Singh, M. D. Johannes, and M. H. Du, Phys. Rev. Lett. **101**, 057003 (2008).
⁵ K. Kuroki, S. Onari, R. Arita, H. Usui, Y. Tanaka, H. Kontani, and H. Aoki, Phys. Rev. Lett. **101**, 087004 (2008).
⁶ K. Seo, B. A. Bernevig, and J. Hu, Phys. Rev. Lett. **101**, 206404 (2008).
⁷ S. Graser, T. A. Maier, P. J. Hirschfeld, and D. J. Scalapino, New J. Phys. **11**, 025016 (2009).
⁸ V. Cvetkovic and Z. Tesanovic, EPL **85**, 37002 (2009).
⁹ A. D. Christianson, E. A. Goremychkin, R. Osborn, S. Rosenkranz, M. D. Lumsden, C. D. Malliakas, I. S.

- Todorov, H. Claus, D. Y. Chung, M. G. Kanatzidis, R. I. Bewley, and T. Guidi, *Nature* **456**, 930 (2008); M.D. Lumsden, A.D. Christianson *J. Phys.: Condens. Matter*, **22**, 203203 (2010).
- ¹⁰ Y. Laplace, J. Bobroff, F. Rullier-Albenque, D. Colson, and A. Forget, *Phys. Rev. B* **80**, 140501(R) (2009).
- ¹¹ R. M. Fernandes, D. K. Pratt, W. Tian, J. Zarestky, A. Kreyssig, S. Nandi, Min Gyu Kim, A. Thaler, Ni Ni, P. C. Canfield, R. J. McQueeney, J. Schmalian, and A. I. Goldman *Phys. Rev. B*, **81**, 140501(R) (2010).
- ¹² A. B. Vorontsov, M. G. Vavilov, and A. V. Chubukov, *Phys. Rev. B* **81**, 174538(2010); R. M. Fernandes, J. Schmalian, *Phys. Rev. B* **82**, 014521(2010).
- ¹³ T. Hanaguri, S. Niitaka, K. Kuroki, H. Takagi, *Science* **328**, 474 (2010).
- ¹⁴ J. Guo, S. Jin, G. Wang, S. Wang, K. Zhu, T. Zhou, M. He, and X. Chen, *Phys. Rev. B* **82**, 180520 (2010).
- ¹⁵ D. F. Agterberg, E. Demler, and B. Janko, *Phys. Rev. B* **66**, 214507 (2002).
- ¹⁶ T. K. Ng and N. Nagaosa, *Europhys. Lett.* **87**, 17003 (2009).
- ¹⁷ J. Linder, I. B. Sperstad, A. Sudbo, *Phys. Rev. B* **80**, 020503(R) (2009).
- ¹⁸ I. B. Sperstad, J. Linder, A. Sudbo, *Phys. Rev. B* **80**, 144507 (2009).
- ¹⁹ V. Stanev and Z. Tešanović, *Phys. Rev. B* **81**, 134522 (2010).
- ²⁰ Y. Ota, M. Machida, T. Koyama, and H. Matsumoto, *Phys. Rev. Lett.* **102**, 237003 (2009); Y. Ota, M. Machida, and T. Koyama, *Phys. Rev. B* **82**, 140509(R) (2010); Y. Ota, M. Machida and T. Koyama, *Phys. Rev. B* **83**, 060503(R) (2011).
- ²¹ E. Berg, N. H. Lindner, and T. Pereg-Barnea, *Phys. Rev. Lett.* **106**, 147003 (2011).
- ²² A.E. Koshelev and V. Stanev, *Europhys. Lett.* **96**, 27014 (2011); V. Stanev and A.E. Koshelev, arXiv:1207.5565.
- ²³ S. Z. Lin, *Phys. Rev. B* **86**, 014510 (2012).
- ²⁴ S. Apostolov and A. Levchenko, arXiv:1210.1875.
- ²⁵ P. Seidel, *Supercond. Sci. Technol.* **24**, 043001 (2011).
- ²⁶ A. I. Buzdin, *Rev. Mod. Phys.* **77**, 935 (2005).
- ²⁷ A. Buzdin and A. E. Koshelev, *Phys. Rev. B* **67**, 220504(R) (2003); H. Sickinger, A. Lipman, M. Weides, R. G. Mints, H. Kohlstedt, D. Koelle, R. Kleiner, and E. Goldobin, *Phys. Rev. Lett.* **109**, 107002 (2012).
- ²⁸ K. Usadel, *Phys. Rev. Lett.* **25**, 560 (1970).
- ²⁹ M. Yu. Kupriyanov and V. F. Lukichev, *Zh. Eksp. Teor. Fiz.* **94**, 139 (1988) [*Sov. Phys. JETP* **67**, 1163 (1988)].
- ³⁰ A. A. Golubov, E. P. Houwman, J. G. Gijsbertsen, V. M. Krasnov, J. Flokstra, H. Rogalla, and M. Yu. Kupriyanov, *Phys. Rev. B* **51**, 1073 (1995).
- ³¹ A. Brinkman, A.A. Golubov, M.Yu. Kupriyanov, *Phys. Rev. B*, **69**, 214407 (2004).
- ³² V. Ambegaokar and A. Baratoff, *Phys. Rev. Lett.* **10**, 486 (1963); A. Barone and G. Paternò, *Physics and Applications of the Josephson Effect*, A Wiley-Interscience Publication, John Wiley & Sons, New York/ Chichester/Brisbane/Toronto/Singapore, 1982, p.52.
- ³³ A.A. Golubov and M. Yu. Kupriyanov, *Pis'ma Zh. Eksp. Teor. Fiz.*, **81**, 419 (2005) [*JETP Lett.* **81**, 335 (2005)].
- ³⁴ Even though, in general, the right hand side of Eq. (39) depends on the ratio of the boundary resistances R_{B1}/R_{B2} , in the transition region this ratio is approximately fixed by the condition $E_{J1} = E_{J2}$ and, as consequence, also mostly depends on bulk parameters.
- ³⁵ V. V. Ryazanov, V. A. Oboznov, A. Yu. Rusanov, A. V. Veretennikov, A. A. Golubov, and J. Aarts, *Phys. Rev. Lett.* **86**, 2427 (2001).
- ³⁶ K. Umezawa, Y. Li, H. Miao, K. Nakayama, Z.-H. Liu, P. Richard, T. Sato, J. B. He, D.-M. Wang, G. F. Chen, H. Ding, T. Takahashi, and S.-C. Wang, *Phys. Rev. Lett.* **108**, 037002 (2012); M. P. Allan, A. W. Rost, A. P. Mackenzie, Yang Xie, J. C. Davis, K. Kihou, C. H. Lee, A. Iyo, H. Eisaki, T.-M. Chuang, *Science* **336**, 563 (2012).
- ³⁷ J. D. Fletcher, A. Serafin, L. Malone, J. G. Analytis, J. H. Chu, A. S. Erickson, I. R. Fisher, and A. Carrington, *Phys. Rev. Lett.* **102**, 147001 (2009); K. Hashimoto, M. Yamashita, S. Kasahara, Y. Senshu, N. Nakata, S. Tonegawa, K. Ikada, A. Serafin, A. Carrington, T. Terashima, H. Ikeda, T. Shibauchi, and Y. Matsuda, *Phys. Rev. B* **81**, 220501(R) (2010).
- ³⁸ P. Richard and T. Sato and K. Nakayama and T. Takahashi and H. Ding, *Rep. Prog. Phys.*, **74** 124512 (2011).